



Practical Approach and Review of Brachial Plexus Pathology With Operative Correlation: What the Radiologist Needs to Know

Sarah E. Stilwill, MD,* Megan K. Mills, MD,* Barry G. Hansford, MD,[†] Hailey Allen, MD,* Mark Mahan, MD,[‡] Kevin R. Moore, MD,[§] and Christopher J. Hanrahan, MD, PhD^{||}

Introduction

The interpretation of brachial plexus imaging studies can be daunting for both the radiology trainee and the practicing general radiologist due to complex anatomy and limited exposure. Familiarity with normal anatomy and a consistent systematic search pattern are critical, as subtle lesions involving the brachial plexus may cause significant detrimental neurologic deficits. Given its associated high spatial and contrast resolution, MRI of the brachial plexus can reveal the location of an abnormality, the extent of nerve involvement and allow the radiologist to come to a succinct differential diagnosis. In the traumatic setting MRI is imperative for preoperative planning.¹⁻⁵ With atraumatic pathology, including tumors, infection, inflammation and radiation plexopathy, recognition of MR characteristics and location of pathology can provide an accurate diagnosis. In this pictorial, case-based review article we describe normal brachial plexus anatomy, present a simple and practical approach to MR imaging interpretation, and present imaging findings of the most common pathology with operative correlation where applicable.

Normal Anatomy

The brachial plexus is a complex network of nerves that supplies the motor and sensory innervation to the upper extremity arising from the ventral nerve roots of C5-T1, which undergo multiple bifurcations and anastomoses, resulting in the five nerve branches (musculocutaneous, ulnar, radial, axillary, and median) to the extremity.⁶ Rarely, C4 or T2 ventral nerve roots may contribute to the brachial plexus, which are termed prefixed and postfixed brachial plexuses.⁷ The postganglionic ventral nerve roots from C5 and C6 give rise to the upper trunk, C7 the middle trunk, and C8 and T1 the lower trunk.⁶ Each trunk divides to give rise to anterior and posterior divisions for a total of 6 divisions.⁶ Divisions then combine into 3 cords with the anterior divisions of the upper and middle trunks forming the lateral cord, the anterior division of the lower trunk forming the middle cord, and the 3 posterior divisions forming the posterior cord.⁶ The cords then give rise to the branches.⁶ Evaluation of the brachial plexus on MRI includes all components from the nerve roots to the level of the branches. Though a mnemonic or two may be helpful to remember the brachial plexus nerve components, having a visual reminder when reading brachial plexus studies is valuable (Fig. 1). Additionally, identification of the roots, trunks, divisions, cords, and branches can be made more manageable through an organized approach, which will be discussed later.

MRI Protocol Considerations

As with any complex anatomy, the MRI protocol used for brachial plexus evaluation is crucial to allow optimal evaluation. This section reviews the field of view, potential sources of artifact, and both basic and advanced sequences that allow visualization of the intricate brachial plexus components.

*Department of Radiology and Imaging Sciences, University of Utah School of Medicine, Salt Lake City, UT.

[†]Department of Diagnostic Radiology, Oregon Health and Science University, Portland, OR.

[‡]Department of Neurosurgery, University of Utah School of Medicine, Salt Lake City, UT.

[§]Intermountain Pediatric Imaging, Primary Children's Hospital, Medical Imaging Department, Salt Lake City, UT.

^{||}Department of Radiology and Imaging Sciences, University of Utah School of Medicine, Salt Lake City, UT.

Address reprint requests to Sarah E. Stilwill MD, University of Utah School of Medicine, Department of Radiology & Imaging Sciences, 30 North 1900 East #1A071, Salt Lake City, UT 84132-2140. E-mails: sarah.stilwill@hsc.utah.edu megan.mills@hsc.utah.edu hansford@ohsu.edu hailey.allen@hsc.utah.edu mark.mahan@hsc.utah.edu kevin.moore@imail.org christopher.hanrahan@hsc.utah.edu

Artifact Minimization

Three major sources of artifact should be considered when imaging the brachial plexus. Commonly encountered artifacts include those due to air–tissue interface, vascular pulsation, and breathing motion. Due to the changing contours of the neck and supraclavicular region, the complex air–tissue interface can contribute to inhomogeneous fat suppression. This can be reduced by the use of Short-*T1* Inversion Recovery (STIR) or Dixon technique that will decrease inhomogeneous fat suppression, especially at high field strength (3T).⁸ Vascular pulsation is best reduced by a saturation band placed over the heart and great vessels that is carefully positioned depending on the plane of the sequence to avoid suppression of the brachial plexus itself or relevant adjacent structures. Respiratory motion artifact is the most difficult to address and is patient-specific. Coaching the patient to avoid heavy breathing can help reduce excessive artifact.

Field of View and Typical Sequences

The field of view should extend from the spinal cord to the lateral axilla effectively covering the root origins to the branches. On coronal imaging, it is helpful to visualize the contralateral nerve roots to the level of the dorsal root ganglion, which can serve as a normal internal comparison. Axial imaging should cover from the level of C4 through the lower axilla. Typical sequences performed include coronal T1 and STIR, axial and sagittal T2 with fat suppression (FS), which can be performed with Dixon or hybrid FS technique to reduce inhomogeneous fat suppression.⁸ At our institution, we also perform a sagittal nonfat suppressed sequence for improved anatomical detail in the costoclavicular space. While brachial plexus MRI with contrast can detect an abnormal blood-nerve barrier, most cases can be performed without contrast. Contrast should be administered in cases where there is concern for tumor, infection, or diffuse involvement.⁶ With patients who are more susceptible to motion due to pain or other reasons, oblique coronal and axial imaging planes can be aligned with the brachial plexus in order to reduce imaging time.⁷ In cases of suspected neurogenic thoracic outlet syndrome, a routine brachial plexus MR is performed with additional sagittal imaging sequences with the arms in neutral position (at the patient's side) as well as the arms abducted (elevated overhead).

Advanced Imaging Sequences

3T imaging is preferred over 1.5T due to the higher signal-to-noise ratio that allows better visualization of nerves. Where available, isotropic 3D STIR or 3D acquisition with Dixon fat suppression can allow for exquisite depiction of the brachial plexus.^{6,9} 3D acquisition also allows for reformatting in various planes and production of maximum intensity projection (MIP) images of the brachial plexus, which can be helpful for radiologist interpretation.⁶

Vascular signal adjacent to brachial plexus structures makes differentiating nerves from adjacent vessels difficult.

Vascular signal is also problematic when attempting to create or interpret coronal STIR MIP images. To reduce the signal from adjacent vessels, sequences have been investigated and shown to provide improved depiction of nerves and/or suppression of adjacent vessel signal. Vascular suppressing sequences include diffusion weighted imaging, 3D diffusion-weighted reversed fast imaging with steady state free suppression, and 3D acquisition with Dixon fat suppression.⁹⁻¹³ Diffusion weighted imaging (DWI) sequences may depict the location of the brachial plexus pathology, but conventional sequences are still typically required to provide a diagnosis or differential diagnosis to the underlying pathology.¹¹

Brachial Plexus MRI—The Approach

Chart Review

Prior to interpretation, careful review of the patients' medical record and pertinent history is crucial for accurate interpretation of brachial plexus MR studies. Correlating with available cervical spine and shoulder imaging studies, electromyography (EMG) reports, physical exam findings, and clinical symptoms can direct the reader to the location of traumatic or atraumatic pathology.

Soft Tissues

Initial assessment of a brachial plexus MR study includes soft tissue evaluation, with careful observation of indirect signs/downstream effects of nerve pathology. The soft tissues, in particular the lower neck and shoulder girdle muscles are evaluated for secondary signs of plexopathy including denervation muscle edema. Denervation muscle edema can be seen in both the acute and chronic setting, with edema signal readily identified on T2 and STIR MR sequences as early as 24 hours following the inciting event and/or injury.¹⁴⁻¹⁶ Edema involving a specific muscle or muscle group can localize the abnormality to the pertinent nerve level within the plexus, and is therefore an important indirect sign that may aid in localizing pathology.^{16,17} Similarly, if postcontrast imaging is available in the acute to subacute setting, the involved musculature will diffusely enhance in a nonmass like fashion, which may be more pronounced than the corresponding findings on fluid-sensitive sequences. Denervation-related muscle volume loss and fatty infiltration take longer to develop and are thus only appreciated in the late subacute-chronic setting.^{14,17} The T1-weighted sequences and nonfat suppressed T2-weighted sequences are the hallmark sequences for demonstrating muscle atrophy.

Anatomical Landmarks

Following soft tissue evaluation, the reader must identify several key anatomical landmarks to guide comprehensive segment-by-segment evaluation of the brachial plexus components. The exit neural foramen is the first key anatomical

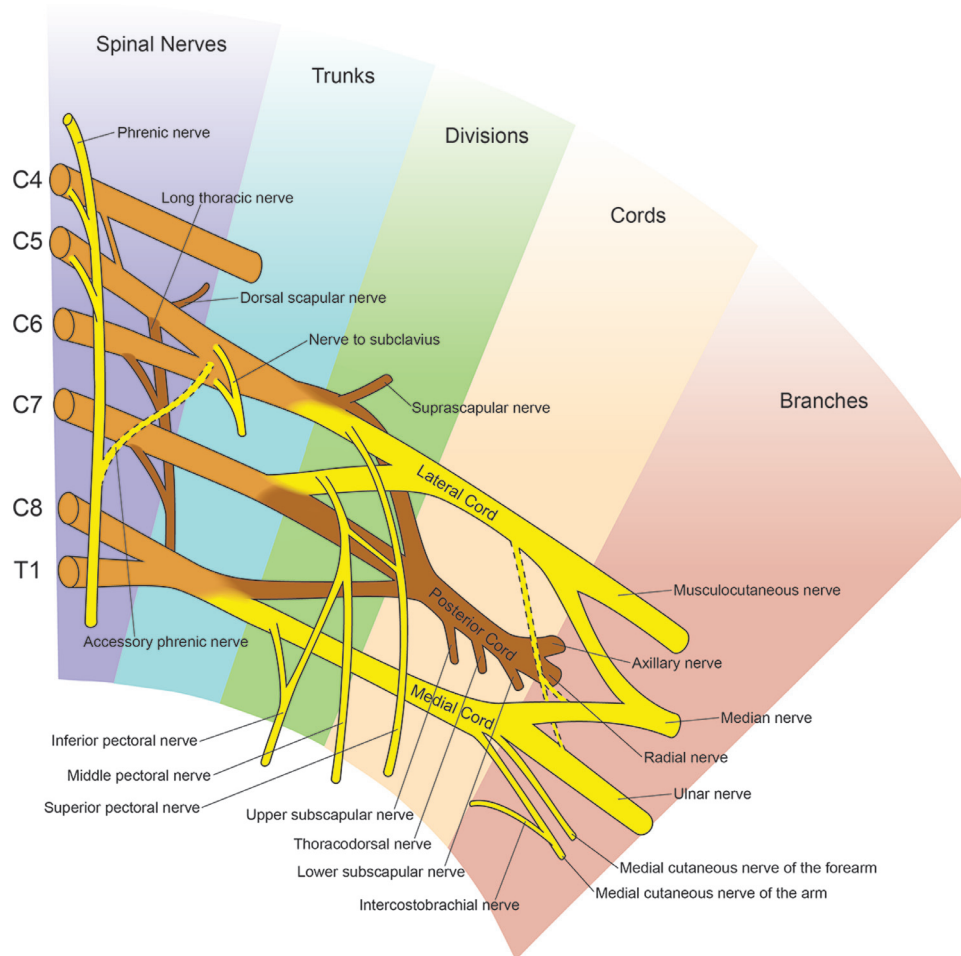


Figure 1 Anatomical representation of the brachial plexus. Illustration of the nerve components and root contributions to the brachial plexus reproduced with permission from the Department of Neurosurgery, University of Utah.

landmark for localization of the spinal nerve roots and their dorsal root ganglia. For pre- and postganglionic nerve root evaluation, the axial T1- and T2-sequences are keys to assess nerve integrity, caliber, and signal with careful attention to the presence of pseudomeningocele formation.¹⁸

Next, the coalescence of the ventral rami to form the brachial plexus trunks is best seen on the axial and sagittal FS T2 Dixon sequences. The trunks extend laterally from the interscalene space, coursing between the anterior and middle scalene muscles (Fig. 2). Lateral to the scalene muscles and above the level of the clavicle (which is the second key anatomical landmark), the brachial plexus trunks form into 6 divisions. The divisions run behind and extend below the level of the clavicle, where they divide into the lateral, posterior and medial cords just distal to the lateral margin of the first rib, (the third key anatomical landmark). The distal divisions and cords are seen readily on the Sagittal T2 FS and non-FS sequences, coursing adjacent to the subclavian artery, an additional key reference point (Fig. 3).¹⁹

Lastly, the cords form the 5 terminal brachial plexus branches at the lateral border of the pectoralis minor muscle, our fourth key anatomical landmark. The median, ulnar,

musculocutaneous, axillary, and radial nerves are seen extending into the axilla, surrounding the axillary artery where they are best appreciated on the coronal T1 and sagittal T2 FS and non-FS sequences (Fig. 4).^{6,18,19}

Sequence-specific evaluation of nerve morphology

The brachial plexus nerves are round or oval in shape, with a smooth contour and uniform fascicular pattern. The nerves are intermediate and/or isointense to skeletal muscle on non-fat suppressed T1- and T2-weighted sequences²⁰ and intermediate to slightly hyperintense in signal on T2 FS/STIR sequences.^{20,21}

The perineural fat signal is preserved on all sequences, but best seen on the T1-sequences. T1 and non-FS T2-sequences best demonstrate perineural fibrosis, variant muscle slips including fibromuscular bands, and the presence of surrounding soft tissue masses.¹⁷ Typically, normal peripheral nerves do not enhance unless there is disruption of the blood-nerve barrier in the setting of tumor, infection, acute inflammation, or following radiation (Table 1).^{6,20}

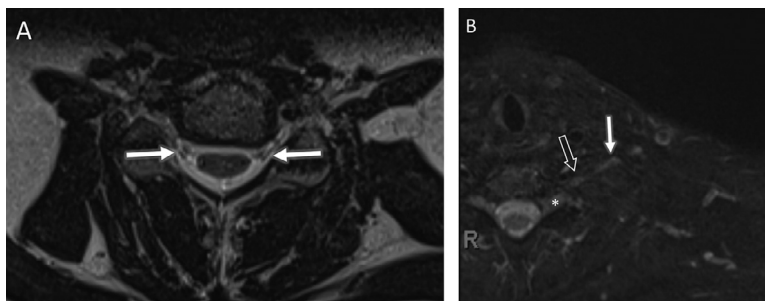


Figure 2 Normal brachial plexus anatomy on MRI: Roots and Trunks. (A) Axial T2 image at the level of C6 shows the preganglionic nerve rootlets (arrows), the first portion of the brachial plexus. The anterior and posterior rootlets coalesce to form the postganglionic nerve root. (B) Axial T2 FS image at the level of the interscalene space show coursing upper trunk (solid white arrow) and C7 nerve root (open arrow) forming the middle trunk, both located between the anterior and middle scalene muscles. The C8 dorsal root ganglion (asterisks) is seen within the exit neural foramen.

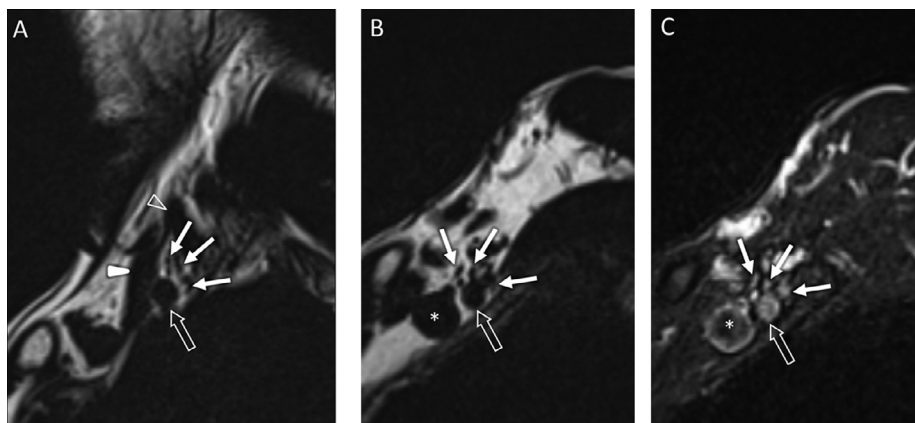


Figure 3 Normal brachial plexus anatomy on MRI: Trunks through Cords. (A) Sagittal T2 Dixon fat-only MR images at the level of the interscalene triangle demonstrates the upper, middle and lower trunks (solid white arrows) emerging between the anterior scalene (white arrowhead) and middle scalene muscles (open white arrowhead), adjacent to the subclavian artery (open white arrows). (B) Sagittal T2 Dixon fat-only MR images at the level of the costoclavicular interval demonstrates the proximal cords including the lateral, posterior, and medial cords (solid white arrows) surrounded by normal hyperintense peri-neural fat coursing adjacent to the subclavian artery (open white arrow) and vein (asterisk). (C) Sagittal T2 Dixon water-only MR image at the same level demonstrates normal morphology of the lateral, posterior, and medial cords (solid white arrows). The nerves are round in shape, with a symmetric fascicular pattern and hyperintense signal with respect to skeletal muscle.

Traumatic Brachial Plexus Injury (BPI)

Nerve Root Avulsions

Traumatic injuries of the brachial plexus can occur anywhere from the proximal nerve root origin to the terminal nerve branches.²² Proximal nerve injuries are typically divided into pre- or postganglionic injuries, categorized by their anatomical relationship to the dorsal root ganglion. The preganglionic segment includes the root entry zone, dorsal and ventral rootlet, intrathecal, and foraminal root. It is vital to distinguish between pre- and postganglionic injury given that location of injury is a major consideration in management decisions.²³⁻²⁵

Preganglionic

Preganglionic nerve root avulsions are most frequently due to traumatic nerve traction with the vast majority of these cases seen in the setting of high velocity motor vehicle accidents.²⁶ The likelihood of avulsion increases with nonclosed vehicles, such as motorcycles, snowmobiles, and all-terrain vehicles. Although less frequent, nerve root avulsion can be caused by lower energy sports-related mechanisms.

Direct imaging findings of preganglionic nerve root avulsion include discontinuity of any portion of the preganglionic segment from the root entry to the dorsal root ganglion.^{25,27} Asymmetric displacement or lateralization of the dorsal root ganglion often results (Fig. 5). The downstream brachial

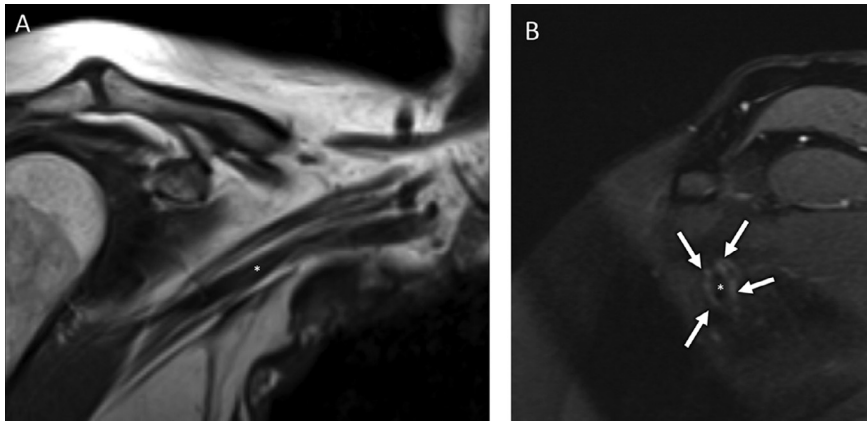


Figure 4 Normal brachial plexus anatomy on MRI: Peripheral Branches. (A) Coronal T1 image demonstrates a normal appearance of the distal most cords, and peripheral branches surrounding the axillary artery (asterisk), extending into the axilla. The distal brachial plexus is best seen on the coronal T1 and sagittal T2 FS and non-FS sequences. (B) Sagittal T2 Dixon water-only image just lateral to the pectoralis minor muscle demonstrates normal appearance of the peripheral branches (solid white arrows), surrounding the axillary artery (asterisk).

Table 1 MR Sequence-Specific Checklist for Assessment of Neural and Perineural Structures

Key Facts:

- ✓ **T1:** Normal anatomy, perineural and intermuscular fat signal, bone marrow signal, chronic fatty muscle infiltration, and methemoglobin blood products.
- ✓ **Fluid sensitive T2/STIR:** Nerve caliber, architecture and signal intensity; perineural, fascicular and muscular edema.
- ✓ **Postcontrast:** + Nerve enhancement in setting of tumor, infection, and acute inflammation; also in functional nerve impairment in setting of traumatic nerve injury.

plexus may show edema and nerve enlargement with signal heterogeneity.²² Contrast-enhanced sequences are not typically necessary to diagnose complete nerve root avulsion, but contrast enhancement of an intact nerve root can signify functional nerve impairment or incomplete injury (Fig. 6).²⁸

CT or MR myelography may be required for diagnosis in cases where preganglionic structures are not well seen on conventional MRI.²⁹ CT myelography was once considered the most reliable modality in identifying preganglionic nerve injury, however, the modality is dependent upon sufficient pooling of cerebrospinal fluid into arachnoid scar and some comparison studies suggest myelography is no better than conventional MRI.^{23,30} MRI provides advantages in the global evaluation for BPI as it includes indirect imaging findings of injury and a more thorough evaluation of the post-ganglionic brachial plexus (Fig. 7).⁵ Advanced imaging techniques such as diffusion-weighted neurography and surface rendered CT have also been proposed as an adjunct to standard MRI to be used in the setting of trauma.⁵

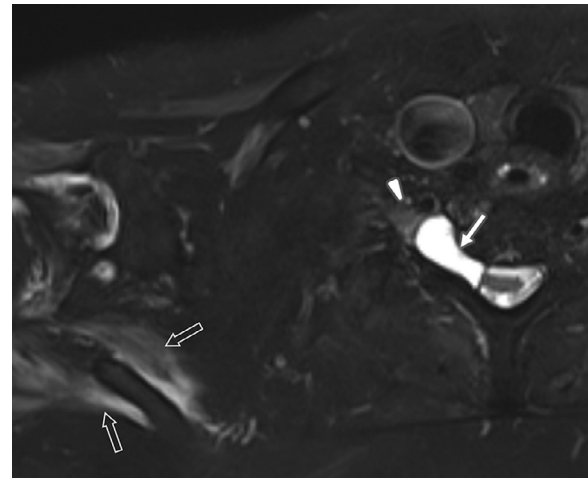


Figure 5 Pre-ganglionic traumatic brachial plexus avulsion injury. 67-year-old man with absent motor function in the right arm, following motorcycle accident 10-months prior to examination. Axial T2 FS MR image through the level of the C7-T1 neural foramen demonstrates a preganglionic nerve root avulsion of C8 (arrowhead) with pseudomeningocele formation (solid white arrow). The C8 nerve is enlarged and laterally displaced. Note the secondary finding of denervation edema in the shoulder girdle musculature (open white arrows).

Indirect imaging findings of preganglionic nerve root avulsion include the development of a pseudomeningocele (Figs. 5-7). Cerebrospinal fluid can fill the void left by the displaced nerve root and while not pathognomonic, this finding should prompt scrutiny of the adjacent neural structures.^{18,22} Unopposed traction from the uninjured contralateral nerves can result in spinal cord displacement away from the side of involvement.^{4,5,27} During the acute or subacute phase of injury, denervation edema can be seen within the involved shoulder girdle and paraspinal muscles or in the arm muscles for upper or lower plexus injury, respectively. Contrast enhancement of involved muscles can occur as early as 24-hours following injury secondary to vascular

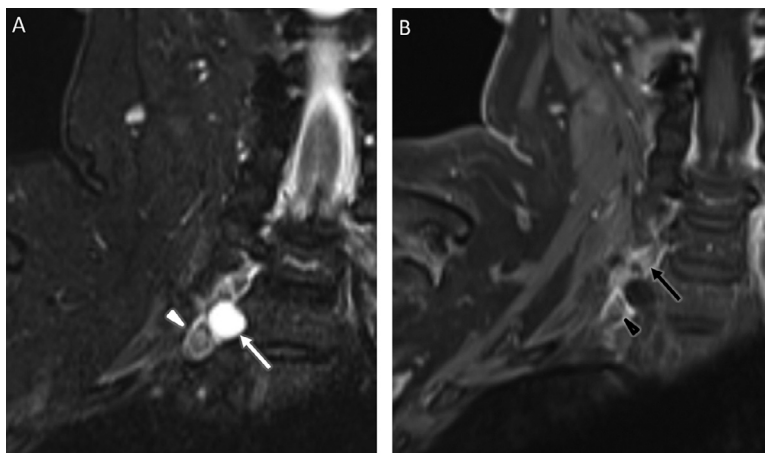


Figure 6 Partial and complete traumatic pre-ganglionic brachial plexus injury. Case images from the same patient presented in Figure 5. (A) Coronal STIR MR image demonstrates the laterally displaced C8 nerve (white arrowhead) and resultant pseudomeningocele formation (white arrow). (B) Coronal T1-weighted post-contrast enhanced MR image with FS at the same level shows enhancement of the avulsed C8 nerve (solid black arrowhead) as well as enhancement of the C7 nerve (solid black arrow) which is seen in continuity. Findings are consistent with complete avulsion of C8 and incomplete, but functional injury of the C7 nerve root.

dilation and increased extracellular space volume.³¹ If left untreated, denervation changes will progress to irreversible chronic muscle atrophy and fatty infiltration (Fig. 8).

A minority of patients with nerve root avulsion may have MRI signal changes in the adjacent cervical spinal cord (Fig. 9). Acutely, cervical spinal cord edema or hemorrhage can be seen, while myelomalacia can develop in the chronic setting.⁵

Preganglionic nerve root avulsions cannot be repaired. Restoring function to the involved extremity is achieved through nerve transfers with particular focus placed on restoration of biceps and shoulder girdle muscle function.^{1,3,5} The treatment approach to preganglionic nerve root injuries can be vastly different than other types of BPI and emphasizes the importance of imaging for injury characterization.

Postganglionic

Postganglionic nerve injuries occur distal to the dorsal root ganglion. Injuries can range from partial stretch injuries to full thickness ruptures or lacerations. While motor vehicle accidents remain the leading cause of injury,² postganglionic injury can occur in any scenario causing inflammation, compression or traction of the brachial plexus.

Direct imaging findings of postganglionic injury include edema and enlargement of the nerve segment involved. In cases of complete transection, discontinuity of the nerve can be seen with eventual neuroma development (Figs. 10–13).³²

Indirect findings include denervation edema of the muscle groups involved. Without restoration of nerve

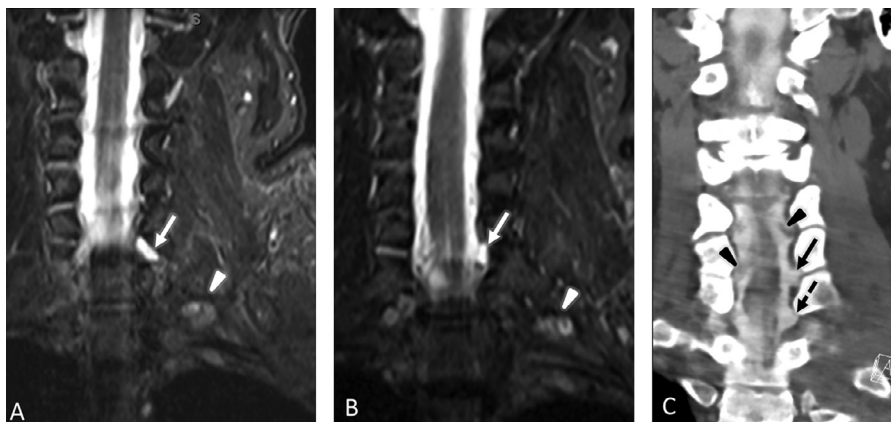


Figure 7 Pre-ganglionic traumatic brachial plexus injury. 41-year-old man with ‘flail arm’ and complete loss of motor function 2-months following a snowmobile accident. (A, B) Sequential coronal STIR MR images show a pseudomeningocele (solid white arrow) with a laterally retracted nerve root, which is redundant and hyperintense (solid white arrowhead). (C) Coronal CT-myelogram in the same patient shows an empty neural foramen at the site of pseudomeningocele formation (solid black arrow). A preganglionic avulsion injury is also present at the level below (dashed black arrow). Note the normal appearance of a more proximal neural foramen containing pre-ganglionic neural structures (solid black arrowheads).

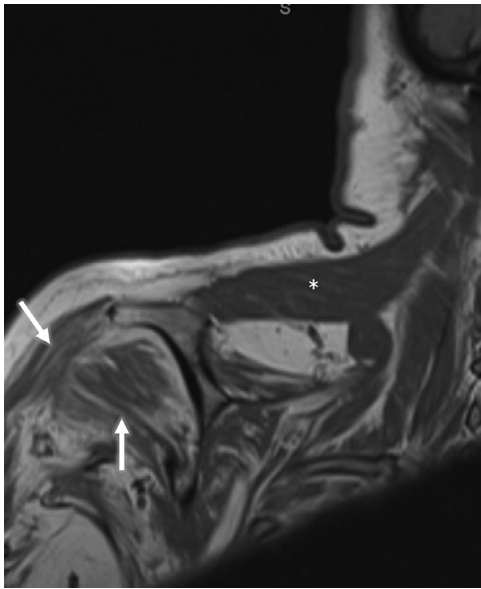


Figure 8 Chronic traumatic BPI. Coronal T1 MR image in the same patient as presented in Figure 5 shows chronic atrophy of the shoulder girdle musculature (solid white arrows). There is relative sparing of the trapezius (asterisk), which is not innervated by the brachial plexus.

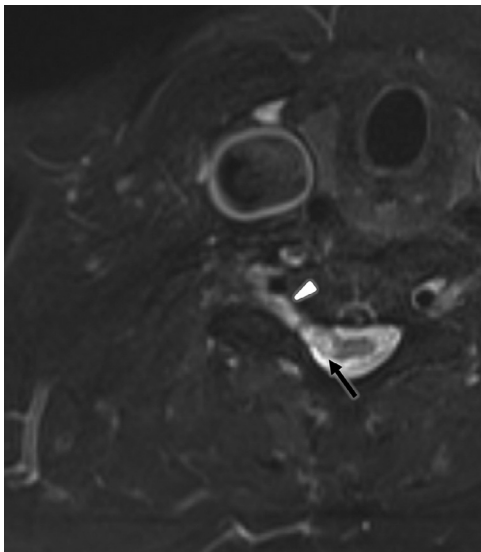


Figure 9 Partial traumatic pre-ganglionic nerve root injury. 65-year-old man status post motorcycle injury 10-months prior. Axial T2 FS MR image shows findings of a partial nerve injury at C6-C7 as evidenced by increased, intrinsic T2 signal heterogeneity of the C7 nerve (white arrowhead) with fiber attenuation. Concomitant signal abnormality of the adjacent hemi-cervical spinal cord is also present (solid black arrow).

conduction, involved muscles eventually progress to chronic atrophy.^{33,34}

Patients with postganglionic injuries have a much better prognosis than their preganglionic counterparts. Most complete postganglionic injuries can be treated with nerve

grafting or distal nerve transfers where incomplete injuries can be managed conservatively.⁵

Peripheral Nerve Injuries

Neuropraxia/Axonotmesis/Neurotmesis

Peripheral nerve injuries have been classified into three types: neuropraxia, axonotmesis, and neurotmesis. These injuries are defined by the histopathology and specific anatomical structures of the nerve unit that are damaged.³⁵

Neuropraxia is a clinical condition hallmarked by temporary loss of function, near complete recovery, and the absence of denervation atrophy of the muscle. It is the mildest form of traumatic plexopathy, that usually resolves in days to within 3 months.³⁵ The nerve is grossly intact in the setting of neuropraxia, but is functionally impaired with slowed or absent conduction in the involved segment.³⁶ Neuropraxia can be caused by multiple mechanisms including traction, compression, or concussion.

Neuropraxia is commonly encountered in collision sports such as American football. Neuropraxia caused by sporting injury is more commonly known as a “burner” or “stinger” reflecting the typical symptomatology of burning sensation in the neck and arm of the affected side immediately following injury.³⁷ While most neuropraxia due to sports injury is transient, usually lasting minutes, recurrent or long-lasting symptoms suggest a more serious injury. Players experiencing one stinger are more likely to experience recurrent neuropraxia which can progress to chronic symptomatology.^{24,38}

Gunshot wounds about the shoulder with complete weakness of the arm are also commonly encountered. Many of these are concussive injuries to the brachial plexus and have good recovery rates with conservative management. The MRI findings in these cases are often subtle.

Treatment of neuropraxia is typically conservative and usually diagnosed clinically. Advanced magnetic resonance imaging may be necessary in cases where symptoms are atypical or prolonged.

Axonotmesis and neurotmesis are more serious injuries involving the axons of the nerve.³⁵ Axonotmesis may still be managed conservatively with a longer expected course of recovery because of Wallerian degeneration and nerve regeneration required to regain function.³² Neurotmesis typically requires surgical intervention due to disruption of not only the axons but the myelin sheath.³²

Imaging in cases of mild neuropraxia can be normal (Fig. 14). Change in size, signal, or course of the nerve can be seen in more severe injuries including axonotmesis. T2 hyperintensity and nerve enlargement are the most common findings with the severity of signal changes often correlating to the severity of the injury (Fig. 15).³²

Given more extensive injury in the setting of neurotmesis, partial or complete nerve disruption can be seen on imaging. Hemorrhage and/or edema, especially in the acute setting, can limit evaluation of the neural structures. Neuroma in continuity or end bulb neuroma may develop at sites of disruption.³²

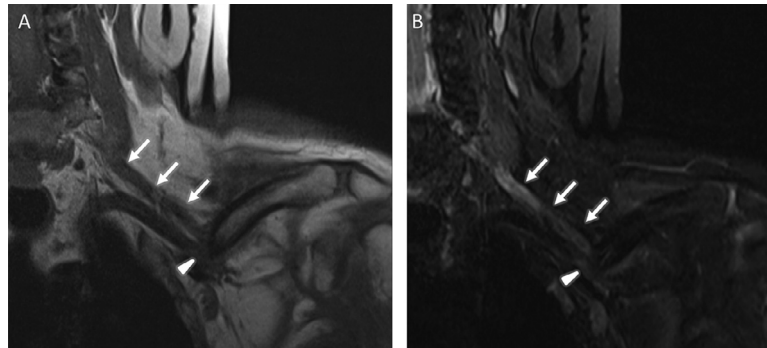


Figure 10 Post-ganglionic traumatic brachial plexus injury. 33-year-old man who presented with a “flail arm” months following polytrauma. (A) Coronal T1-weighted MR image and (B) Coronal STIR MR image show a displaced left clavicle fracture, which impinges and partially transects the coursing brachial plexus at the level of the distal divisions / proximal cords (white arrowhead). There is marked edema and enlargement of the upper trunk (solid white arrows).

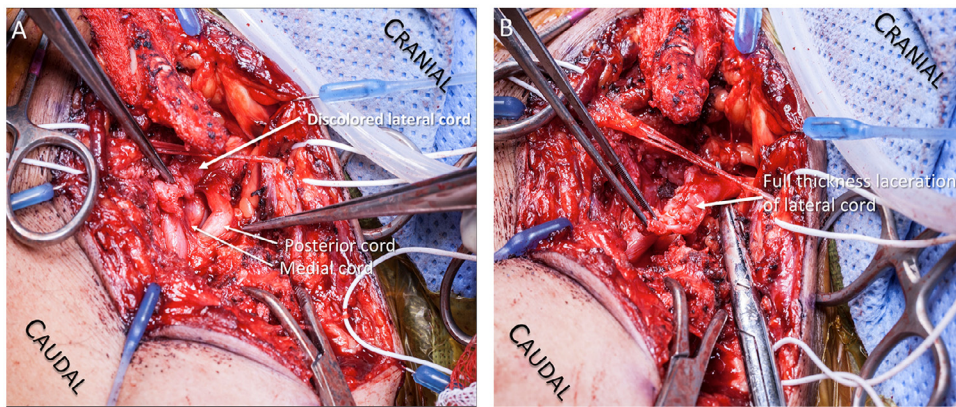


Figure 11 Full-thickness BP laceration injury: Intra-operative view. 40-year-old male presented with a mid-shaft clavicle fracture and lateral cord distribution neurologic deficits following motorcycle crash. (A) Intra-operative view of the base of neck demonstrates a discolored lateral cord, and normal gross appearance of the adjacent posterior and medial cords. (B) With deeper intra-operative exploration, full-thickness laceration of the lateral cord is apparent with proximal nerve swelling visible at the location of the tenotomy scissors.

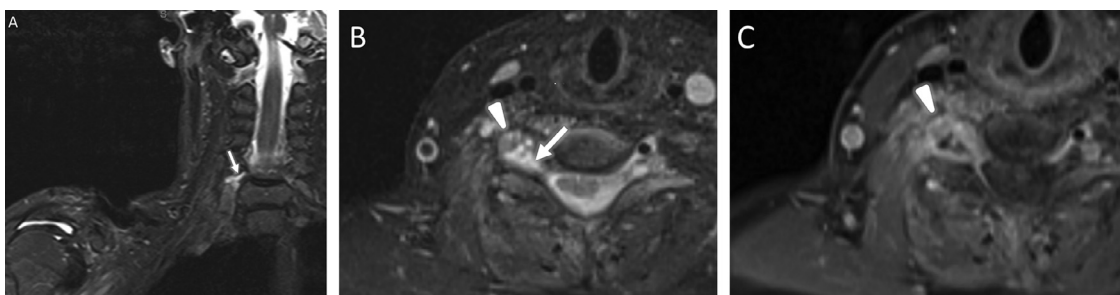


Figure 12 Pre-ganglionic traumatic brachial plexus injury. 47-year-old woman who had complete motor loss above the level of the wrist following a motorcycle/moose collision. Patient exam and EMG findings were diagnostic of an upper plexus injury with involvement in the upper and middle trunks but some preserved function in the lower trunk. (A) Coronal STIR MR image shows pseudomeningocele formation (solid white arrow) consistent with pre-ganglionic nerve root avulsion injury. (B) Axial T2-weighted MR image shows the pseudomeningocele (solid white arrow) as well as a laterally displaced and redundant nerve (white arrowhead). (C) Axial T1-weighted post-contrast FS sequence shows enhancement of the retracted nerve (white arrowhead).

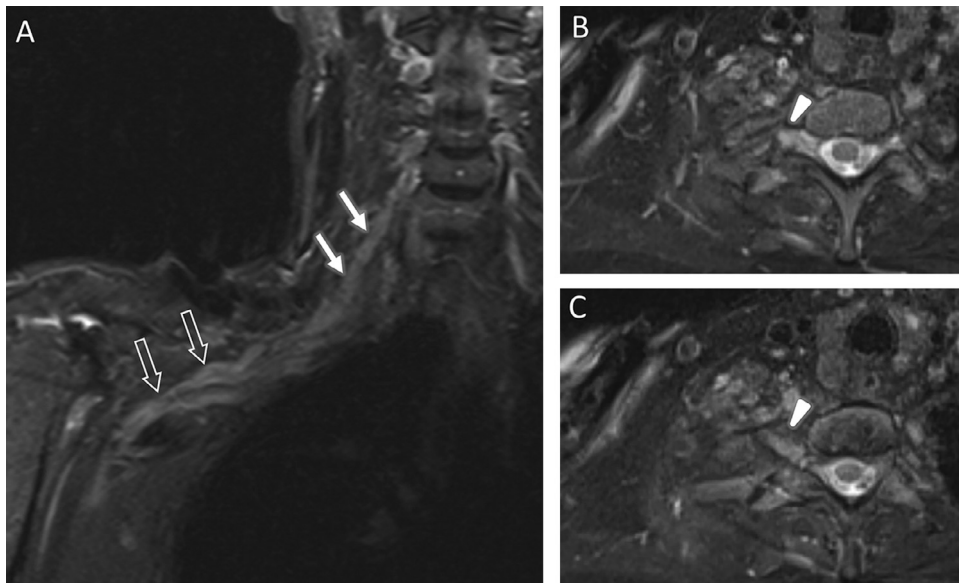


Figure 13 Concomitant traumatic post-ganglionic brachial plexus injury in the same patient as presented in Figure 12. (A) Coronal STIR MR image shows enlargement and edema of multiple portions of the upper brachial plexus consistent with post-ganglionic injury. The C5 root and upper trunk (solid white arrows) as well as the cords (open white arrows) are involved. Ax T2 FS images immediately above (B) and below (C) the level of the preganglionic nerve avulsion injury (depicted in Figure 12) demonstrate intact, but edematous nerve roots (arrowheads).

Brachial Plexus Birth Palsy

Brachial plexus birth palsy (also known as birth palsy) is a traumatic brachial plexus injury that occurs secondary to excessive traction on the plexus during difficult delivery, often in the setting of breech presentation or forceps-assisted delivery. The underlying mechanism is brachial plexus stretch or avulsion from the spinal cord.^{39,40} Brachial plexus birth-related traction injuries may involve the upper plexus (C5 and C6 nerve roots) producing the classic Erb-Duchenne palsy (40%), the lower plexus (C8 and T1 nerve roots) resulting in a Klumpke palsy (30%), or both upper and lower neural elements (total plexus injury, 30%).³⁹⁻⁴¹ Injury may occur proximal (preganglionic) to

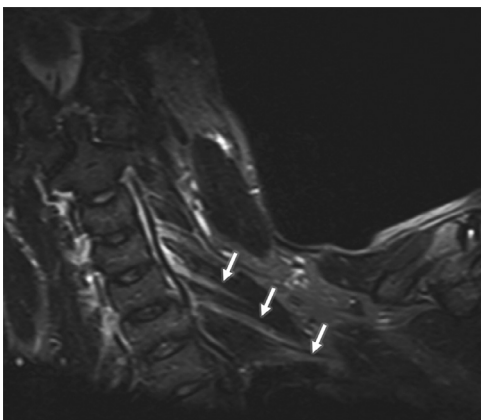


Figure 14 Transient Neuropraxia. 21-year-old male football player who sustained multiple 'stingers' with normal MR imaging findings in the setting of transient neuropraxia. Coronal STIR MR image demonstrates normal size and signal intensity of the imaged brachial plexus roots and trunks (solid white arrows). The patient was treated conservatively and symptomatology resolved.

the dorsal root ganglion resulting in partial or total nerve root avulsion, or distal (post-ganglionic) to the dorsal root ganglion leading to traumatic neuroma formation.³⁹⁻⁴¹

Imaging Findings

Preganglionic Injury

Similar to the adult traumatic injury, nerve roots are avulsed from the spinal cord with concurrent nerve sheath injury,

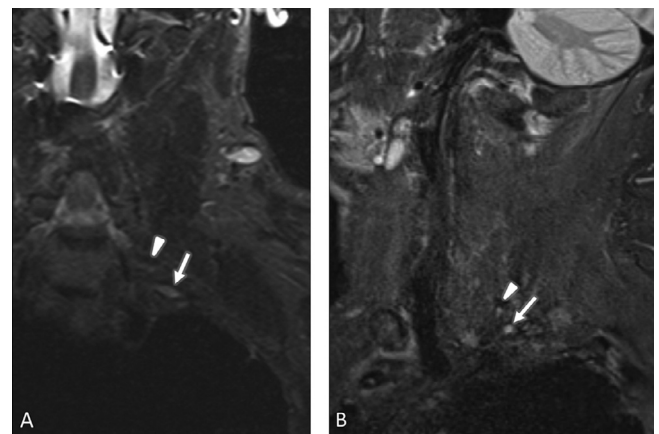


Figure 15 Idiopathic lower trunk brachial plexus injury. 54-year-old man who presented with persistent lateral 4th and 5th digit numbness without history of injury. The patient had clinical and EMG findings consistent with a lower trunk plexopathy. (A) Coronal STIR MR and (B) Sagittal T2-weighted FS MR images demonstrate enlargement and hyperintense signal in the left C8 nerve root (solid white arrow) and lower trunk. Compare the abnormal C8 nerve (solid white arrow) with the adjacent, normal C7 nerve root (white arrowhead).

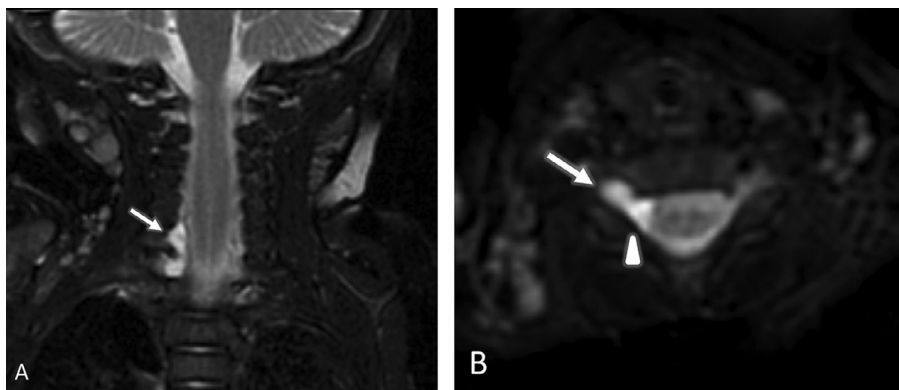


Figure 16 Brachial plexus birth palsy/obstetrical brachial plexus palsy (OBPP)- Preganglionic traction injury with avulsion pseudomeningocele. 3-month-old baby with right arm Erb’s palsy since birth. (A) Coronal STIR MR demonstrates an extradural fluid collection (solid white arrow) without intrinsic neural elements following C6 and C7 root avulsion. (B) Axial STIR MR image confirms absence of neural elements within the avulsion pseudomeningocele (solid white arrow). The extradural fluid (white arrowhead) produces mild mass effect on the dural sac.

resulting in a pseudomeningocele, which does not contain nerve roots (Fig. 16).³⁹⁻⁴² Attenuated or disrupted proximal roots and/or rami within or immediately distal to diverticulum may contract into a nerve “retraction ball,” which can also occur in distal nerve elements. Denervation changes in posterior cervical paraspinal muscles (especially multifidus) usually reflect a preganglionic injury. Spinal cord edema, myelomalacia, and syringomyelia are possible. Central spinal cord edema is seen in the acute stage, secondary to root avulsion.³⁹⁻⁴²

Postganglionic Injury

Stretch injury results in variable enlargement or attenuation of the stretched (but anatomically contiguous) plexus elements. Local soft tissue edema and muscle denervation changes in the distribution of the injured neural elements are

common (Fig. 17). Chronic injury may show enhancing scar tissue within the stretched neural elements. Enhancing muscle implies ongoing denervation.³⁹⁻⁴²

Glenohumeral dysplasia also occurs as a sequelae of brachial plexopathy on the developing glenoid and humeral head. Imaging reveals a dysplastic glenoid, winged scapula, and hooked coracoid. The humeral head is small and ovoid.^{40,41,43}

Clinical Findings

Clinical findings depend on the severity and distribution of plexus injury. Injury to one or more brachial plexus nerve roots, trunks, or cords leads to upper extremity contracture. Complete brachial plexus avulsion produces a useless “flail arm.” Note that clinically incomplete paralysis is commonly observed even with complete root avulsion(s) because of

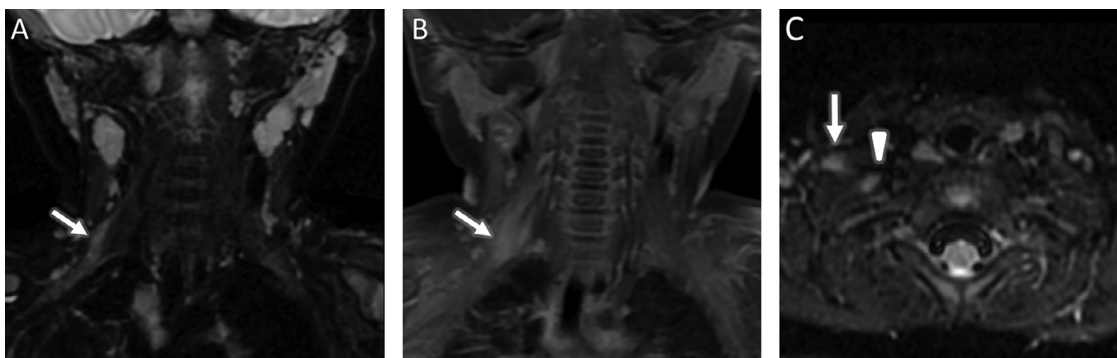


Figure 17 OBPP- Postganglionic traction injury. Full term 5-month-old baby who had failed descent during birth, delivered with traction, with immediate right upper extremity palsy and no functional recovery since birth. (A) Coronal STIR MR image depicts abnormal thickening and hyperintensity of the upper trunk (solid white arrow) with concordant attenuation of the proximal C5 ventral primary ramus. (B) Coronal T1 post contrast FS MR image shows avid amorphous enhancement of the upper trunk (solid white arrow) as well as the contributing neural elements and surrounding tissue reflecting blood-neural barrier disruption within the retraction neuroma and local scar tissue formation. (C) Axial STIR MR image shows abnormal enlargement of the upper (solid white arrow) and middle trunk (white arrowhead) as they pass through the scalene triangle.

redundant muscle innervation from multiple roots. The most common signs and/or symptoms include extremity pain, paralysis of the ipsilateral limb with or without phrenic nerve palsy. The clinical examination cannot reliably distinguish between pre- and postganglionic injuries.⁴⁰

Clinically, the classic Erb-Duchenne palsy results from upper plexus injury (C5, C6 roots, upper trunk) during forced adduction and downward traction resulting in proximal muscle weakness with loss of shoulder abduction, shoulder external rotation, elbow flexion, and forearm supination.^{40,44,45} This is the most common obstetrical brachial plexus palsy traction injury pattern. The less common Klumpke palsy results from forced abduction and upward traction on the arm to the lower plexus (C8, T1 roots, lower trunk) resulting in distal muscle weakness with hand paralysis.^{40,44,45}

Accurate characterization of injury level is critical to treatment planning and prognosis. In general, birth plexus injuries tend to have better functional outcomes than similar injuries in adult patients.

At surgery, the surgeon may find evidence for root avulsion, neuroma, spinal cord displacement or edema, hemorrhage or scarring in the spinal canal, absence of nerve roots within the intervertebral foramina, and/or pseudomeningocele(s) (Fig. 18).³⁹⁻⁴² Operative brachial plexus exploration and intervention is based on a combination of clinical and imaging findings. Nerve grafting or nerve transfers are performed to improve clinical function when axonal regeneration and distal re-innervation is inadequate. Scar tissue formation (neuroma) at the site of traction injury is resected in the setting of nerve grafting so interposed nerves can act as a conduit to reach their distal target without interruption (Fig. 19).^{46,47} Nerve transfers are used in the setting of multiple nerve root avulsions, in which a functioning nerve is used to innervate a distal target.^{46,47}

Nontraumatic Brachial Plexus Pathology

Radiation-Induced Brachial Plexopathy

Patients who have received radiation therapy directed to the lower neck, upper back, upper lung, and pectoral girdle may develop symptomatic brachial plexopathy. The underlying pathophysiology of radiation-induced plexopathy is not well understood, although oxidative stress and alterations in microvascular blood supply leading to fibroblast proliferation with eventual neural and perineural fibrosis are thought to be involved.⁴⁸

Patients can present with pain, weakness, loss of sensation or altered sensation in the distribution of the affected nerves. The at-risk population includes patients radiated for breast cancer, lung cancer, laryngeal or glottic cancer, lymphoma, and localized metastases of the bones or soft tissues in the region of the plexus.^{25,48} The likelihood of developing radiation plexopathy is dose dependent, with an incidence of approximately 5%-10% among patients receiving at least 60 Gy to the lower neck or upper chest. Signs and symptoms of plexopathy can be seen at lower doses (50 Gy) if the patient has also undergone surgery in the region of the plexus.^{6,49}

The latent period from the time of treatment completion to symptom onset is markedly variable, with early cases presenting within a few months of treatment and other patients presenting up to two decades later.⁵⁰ Kori et al reported an average latency of 5 years with a median of 4 years.⁴⁹

The role of MRI in these patients is to help distinguish between radiation plexopathy and recurrence of tumor, as the clinical findings may be similar. Nerves affected by radiation can be focally or diffusely enlarged with increased signal on STIR/T2-weighted images (Fig. 20).^{50,51} Perineural fibrosis appears as T1 and T2 hypointense signal surrounding or encasing the plexus structures.²⁵ Tension from the fibrosis can

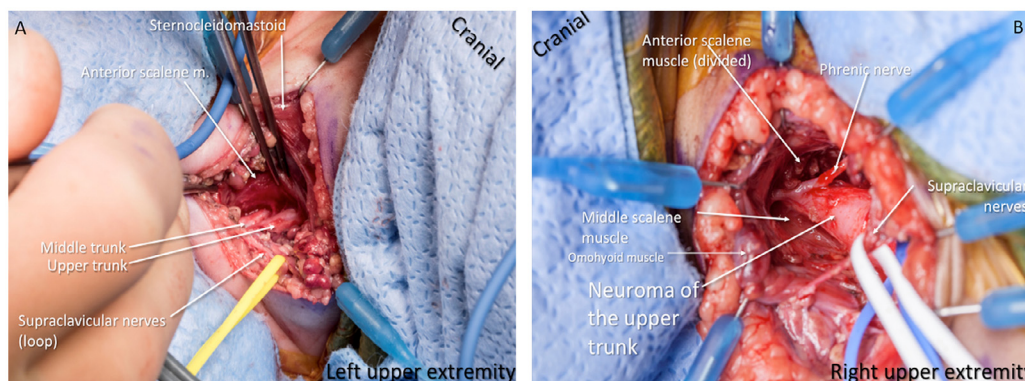


Figure 18 OBPP- Normal vs. abnormal intra-operative view of BP. Case images from patient presented in Figure 17. (A) Intra-operative view of the left base of neck during exploration for contralateral C7 transfer (donor side) demonstrates normal appearance of the coursing upper and middle trunks, with retraction of the sternocleidomastoid and anterior scalene muscles. (B) Intra-operative view of the contra-lateral, right base of neck demonstrates abnormal appearance of the brachial plexus with neuroma formation of the upper trunk. The anterior scalene muscle has been divided during exploration.

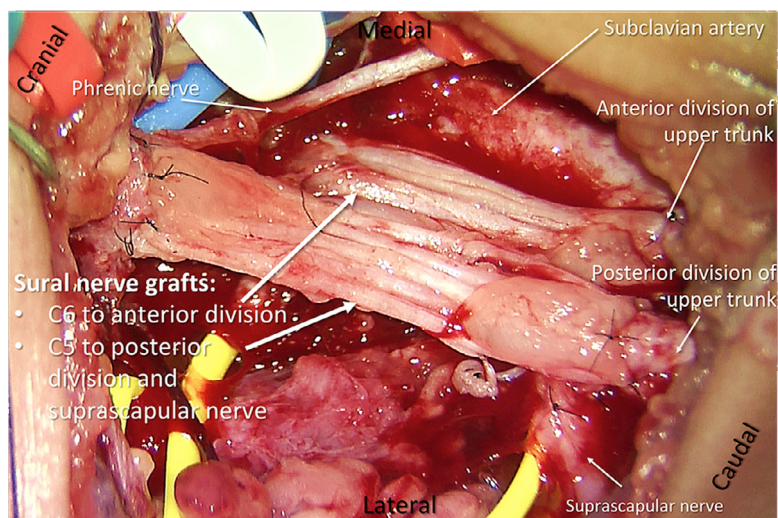


Figure 19 OBPP- Intra-operative microscopic view of a nerve graft procedure. Surgical repair of the neonatal brachial plexus palsy visualized in prior figure 18. The neuroma of the upper trunk was resected and the C5 and C6 roots were trimmed back to normal fascicular appearance. Similarly, the distal portion of the upper trunk was trimmed back to healthy nerve. Multicable nerve grafts were used to coapt (connect) C5 root to the posterior division of the upper trunk and suprascapular nerve, and from the C6 root to the anterior division of the upper trunk. Fibrin glue has been placed on the suture coaptation sites to augment the suture repair.

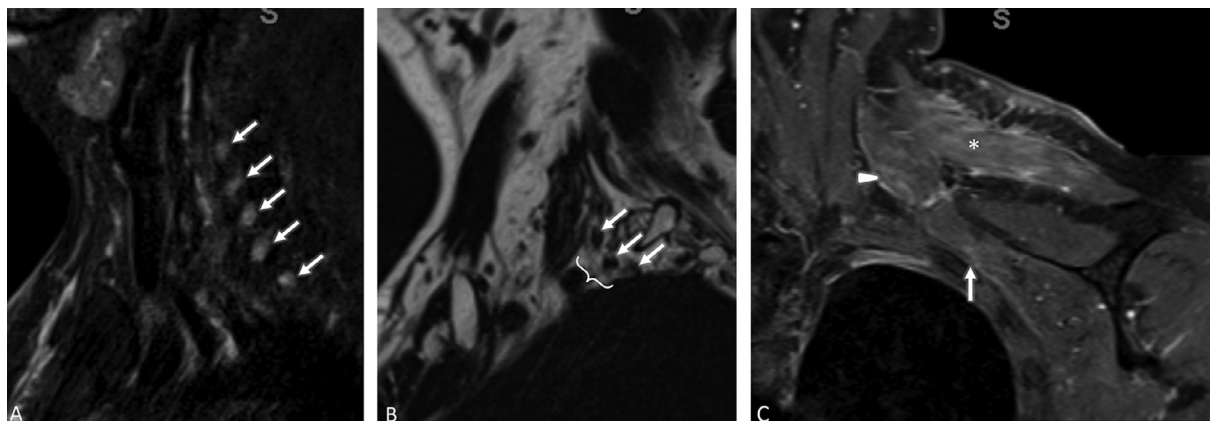


Figure 20 Radiation Plexopathy. 67-year old woman status post 60 Gy of external beam radiation therapy directed to the left chest wall, axilla and left supraclavicular region for recurrent breast cancer. (A) Sagittal T2 Dixon water-specific MR image demonstrates enlargement and T2 hyperintensity of the C5-T1 nerve roots (solid white arrows). (B) Sagittal T2 Dixon fat-specific MR image reveals mild hypointense stranding of the peri-neural fat (bracket) surrounding the brachial plexus trunks (solid white arrows), compatible with mild/ early peri-neural fibrosis.(C) Coronal T1 FS post-contrast image of the brachial plexus depicts mildly enhancing muscle edema involving the left trapezius (asterisk), posterior scalene (solid white arrowhead) and serratus anterior (solid white arrow), related to both direct effects of the radiotherapy and indirect denervation edema.

result in distortion or focal angulation of the nerves. Abnormal findings should be limited to the radiation field, the extent of which can sometimes be deduced by patterns of fatty replacement of the marrow or geographic edema of the muscles and soft tissues.⁵¹ Postcontrast images can demonstrate mild generalized enhancement of the affected nerves whereas mass-like or nodular enhancement would be inconsistent with radiation-related effects and would more likely indicate recurrent malignancy or perineural spread of tumor.⁵⁰ In contrast to tumor

recurrence, imaging findings of radiation plexopathy tend to be stable across serial examinations.⁵¹

Thoracic Outlet Syndrome

Compression of the neurovascular bundle of the upper extremity within the interscalene triangle, costoclavicular interval, or retropectoralis minor space can result in thoracic outlet syndrome (TOS). The most common type of TOS is

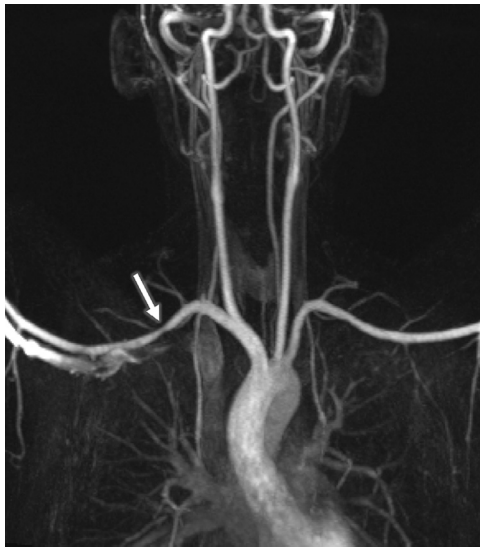


Figure 21 Thoracic Outlet Syndrome (TOS). 27-year-old woman with vasculogenic thoracic outlet syndrome, presenting with aching and tingling in her right upper extremity during overhead arm positioning. Coronal maximum intensity projection (MIP) image of the chest from MR angiogram (arterial phase) demonstrates focal narrowing of the right subclavian artery (solid white arrow) with arms in the abducted position. For comparison, the left subclavian artery is normal in caliber.

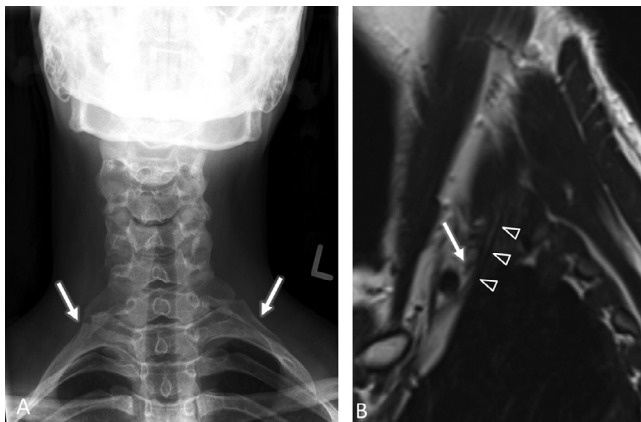


Figure 22 TOS secondary to cervical ribs. 35-year-old man presents with right upper extremity numbness, and pain at the base of the neck. (A) AP radiograph of the cervical spine depicting bilateral cervical ribs arising from C7 (solid white arrows). (B) Sagittal T2 Dixon fat-specific MR image with arms in the abducted position demonstrates the cervical rib (open white arrowheads) abutting and slightly displacing the lower trunk of the plexus (solid white arrow).

vasculogenic, wherein the subclavian and/or axillary vein, artery, or both are compressed.^{52,53} Patients present with pain, swelling, numbness, alterations in skin temperature, and skin discoloration, which is typically worsened by arm abduction or overhead activities. Vascular thrombosis, venous collateralization, and aneurysm formation can be seen in severe cases. True neurogenic TOS, caused by

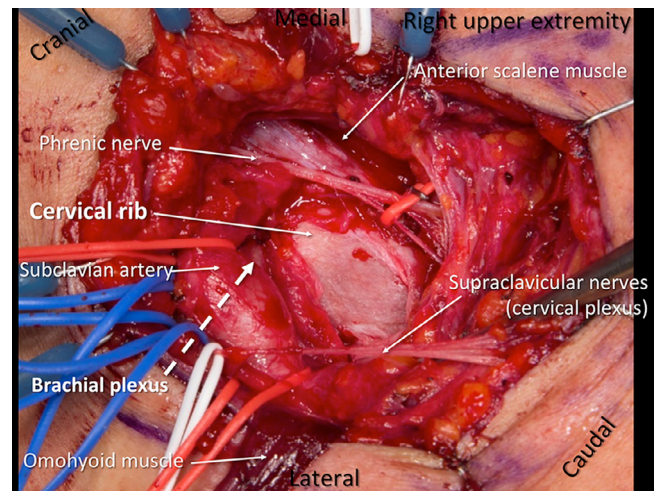


Figure 23 Cervical Rib- Intra-operative view. Surgical resection of cervical rib that was fused to the first thoracic rib. Notable intra-operative findings include a subclavian artery cranial to the cervical rib (and substantially rostral to the clavicle which is not visualized below the supraclavicular nerves). The brachial plexus (dashed white arrow) is obscured and posteriorly displaced by the cervical rib and subclavian artery. The anterior scalene muscle is atrophic and largely fibrotic.

compression of the brachial plexus as it traverses the thoracic outlet, is significantly less common. Patients with neurogenic TOS typically present with painless neurologic loss, including atrophy and numbness of the hand and medial forearm.^{52,53} The so-called disputed neurogenic TOS is a pain syndrome with subjective numbness in a lower trunk pattern and pain in the periscapular and lateral neck region. It is classically triggered with dynamic movements and overhead arm positioning. Compression of the brachial plexus in such cases involves the lower trunk resulting in ulnar sided symptoms 68% of the time, with both ulnar and radial symptoms or isolated radial sided symptoms occurring less frequently (20% and 12% of the time, respectively).^{52,53}

Potential causes of neurovascular compression leading to TOS are numerous and include: cervical rib, elongated C7 transverse process, abnormal first rib, anomalous muscle, hypertrophied anterior scalene muscle, anomalous blood vessels, intramuscular course of brachial plexus structures, and anomalous fibromuscular bands.^{25,52,54}

Imaging evaluation of patients with suspected TOS should include radiographs of the cervical spine and/or chest to assess for rib and other osseous abnormalities. Multiphase MR angiography and dynamic and/or positional imaging of the brachial plexus are included in the MR evaluation of patients with suspected TOS at our institution.⁵²⁻⁵⁴ Mild flattening of the subclavian vein with arm abduction is a normal finding, however the subclavian artery should maintain a round, noncompressible morphology (Fig. 21). Significant flattening of the subclavian vein of more than 50% of the vessel caliber would be considered abnormal, particularly if asymmetric to the asymptomatic side. The course of the plexus should be assessed

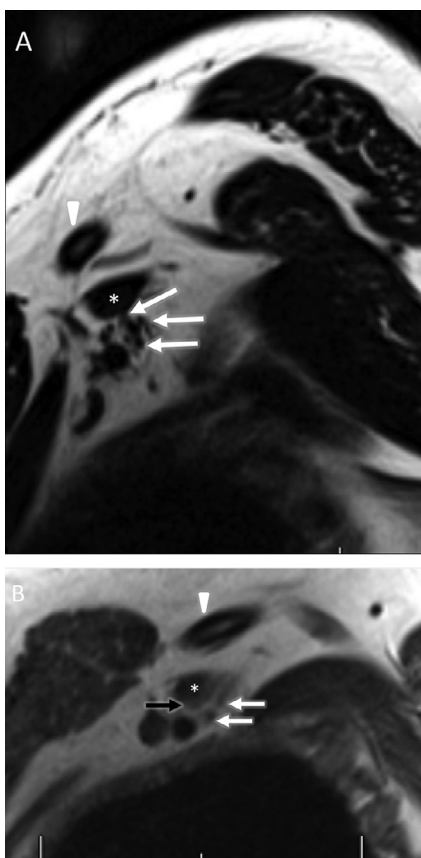


Figure 24 Subclavius posticus muscle. 47-year-old woman with left upper extremity numbness found to have an anomalous subclavius posticus muscle. (A) Sagittal T2 Dixon fat-specific MR image with arms in neutral position. The anomalous muscle (asterisk) originates from the first rib and inserts upon the superior angle of the scapula running in an AP oblique plane. The lateral, posterior and medial cords of the plexus run slightly inferior and posterior to the anomalous muscle (solid white arrows). (B) Sagittal T2 Dixon fat-specific MR image with arms in dynamic abduction position with subtle inferior displacement of the nerves by the anomalous muscle (asterisk). The muscle directly abuts the lateral cord (solid black arrow). The posterior and medial cords of the plexus run slightly more inferior and posterior to the muscle (solid white arrows). The clavicle is located superiorly (white arrowhead).

for abutment or compression by adjacent osseous structures and for loss of intervening fat planes, particularly with the arms abducted (Figs. 22 and 23). The identification of focal displacement of the plexus, nerve kinking or loss of the normal oval and/or round shape of the brachial plexus structures should lead to further interrogation for a subtle fibrous band or anomalous muscle (Fig. 24).⁵²⁻⁵⁴

Brachial Plexitis—Parsonage Turner Syndrome

An uncommon cause of brachial plexus dysfunction is idiopathic brachial plexitis, also known as Parsonage-Turner syndrome or neuralgic amyotrophy. Patients present with

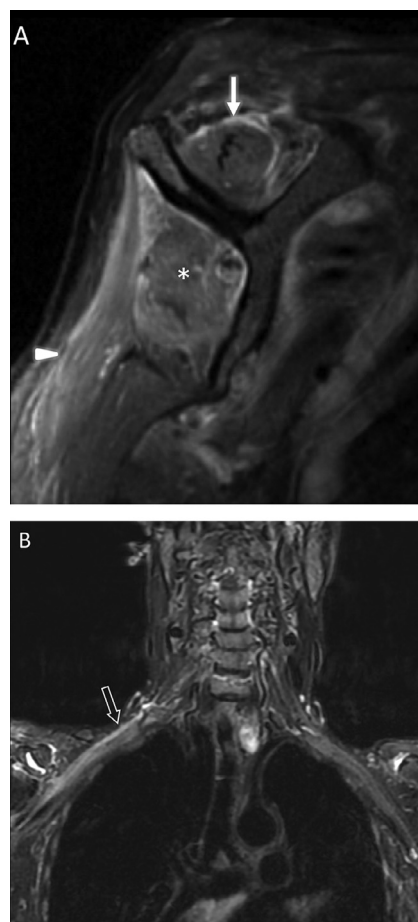


Figure 25 Parsonage Turner Syndrome. 71-year-old-woman presents with sudden onset, severe right upper extremity pain. (A) Sagittal T2 FS MR image of the right shoulder demonstrates multi-compartment muscle edema involving the distribution of both the supra-scapular and long dorsal thoracic nerves. There is denervation muscle edema within the supraspinatus (solid white arrow), infraspinatus (asterisk) and deltoid muscles (white arrowhead). (B) Coronal T2 FS MR image through the upper chest reveals marked hyperintensity and mild asymmetric enlargement of the coursing brachial plexus (open white arrow) consistent with acute neuritis.

sudden onset severe pain involving one or both upper extremities followed by progressive motor weakness and sensory dysfunction. It is more commonly seen in patients with a recent history of trauma, viral infection, vaccination, or surgery and is believed to be autoimmune in etiology although specifics of its pathophysiology remain unknown.⁵⁵

While Parsonage-Turner syndrome is primarily a clinical diagnosis, MRI of the brachial plexus or shoulder can be performed to assess for other possible etiologies of symptoms and to characterize the extent and distribution of abnormal findings.⁵⁵ Indirect signs predominate on MRI, with multi-compartmental feathery denervation muscle edema being the most common finding (Fig. 25). Direct signs of neuropathy, specifically nerve enlargement and increased T2/STIR signal intensity, may also be present.^{16,56}

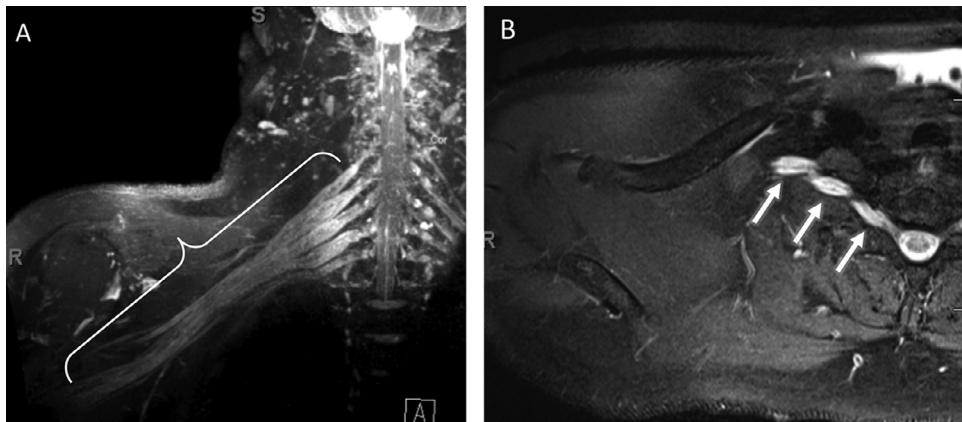


Figure 26 Chronic inflammatory demyelinating plexopathy (CIDP). 47-year-old man presenting with slowly progressive numbness, weakness, and loss of coordination of his right upper extremity. (A) Coronal 3D SPACE maximum intensity projection (MIP) MR image of the right brachial plexus demonstrates marked enlargement and T2 hyperintensity of the brachial plexus from the roots to the proximal branches (bracket). (B) Ax T2 FS MR image through the roots and trunks demonstrate similar findings of nerve hypertrophy and diffuse increased intrinsic hyperintense signal (solid white arrows). The partially imaged left brachial plexus are normal in caliber and signal.

Chronic Inflammatory Demyelinating Polyneuropathy

Chronic inflammatory demyelinating polyneuropathy (CIDP) is a rare autoimmune neuropathy that can involve the brachial or lumbosacral plexus. Patients present with progressive motor weakness involving proximal and distal muscles that lasts more than 8 weeks.⁵⁷ Sensory symptoms of numbness and pain can also be seen. CIDP can be monophasic or relapsing, and treatment typically involves immune modulation therapy (intravenous immunoglobulin and corticosteroids).^{58,59} MRI demonstrates marked hypertrophy of the brachial plexus structures with associated T2/STIR hyperintensity (Fig. 26).⁶⁰ Findings are classically symmetric, although unilateral cases are possible.^{60,61} In some cases, the severe hypertrophy of the roots and proximal trunks can result in an “onion bulb” morphology of the plexus, as can be seen in the congenital hypertrophic neuropathy Charcot-Marie-Tooth disease. Prolonged or relapsing cases of CIDP can also be associated with profound muscle atrophy.⁶¹

Infection

Infectious brachial neuritis is relatively uncommon, however when it does occur, it is most commonly due to a direct spread of infection from adjacent soft tissues. There are a few reported cases in the literature of secondary infection of the brachial plexus related to septic glenohumeral arthropathy, spinal osteomyelitis-discitis, apical lung pleural and/or parenchymal infection, overlying soft tissue infections, recent surgery, or postvenous catheter line placement (septic thrombophlebitis).^{62,63} MRI findings of infectious neuritis are similar to other sites of soft tissue infection and include nonmass like enhancement, increased intrinsic T2-hyperintense signal of the involved nerve and/or nerve

fascicles, and adjacent soft tissue inflammation. Imaging may or may not demonstrate the inciting source and/or site of infection spreading to the coursing brachial plexus (Fig. 27).^{27,62-64}

Tumors of the Brachial Plexus

Malignant involvement of the brachial plexus is not a rare occurrence and is most often seen secondary to invasion from adjacent apical lung cancer, breast cancer, lymphadenopathy, primary bone tumors, or metastases. In contradistinction, primary tumors of the brachial plexus, both benign and malignant, are rare and broadly divided into tumors of neurogenic vs non-neurogenic origin.⁶⁵ MRI is the preferred imaging modality for evaluating tumors of the brachial plexus with PET and CT useful adjuncts for problem-solving and preoperative planning. When combining lesion-specific imaging features with clinical presentation and past medical history, it is often possible to provide a limited differential or specific diagnosis.

Neurogenic Tumors

Neurogenic tumors of the brachial plexus are further classified as benign vs malignant. Benign entities include schwannoma, neurofibroma, ganglioneuroma, and plexiform neurofibroma. Although plexiform neurofibroma is considered benign, there is an increased risk of malignant transformation with estimates ranging from 5%-10% in large tumors.⁶⁶ The primary malignant tumor of the brachial plexus is a malignant peripheral nerve sheath tumor (MPNST). When evaluating tumors of the brachial plexus, it is important to consider underlying medical conditions as plexiform neurofibromas and neurofibromas occur at



Figure 27 Septic Thrombophlebitis. 28 -year-old female, IV drug user with worsening shoulder pain. (A) Right upper extremity ultrasound demonstrates acute thrombus within the proximal brachial vein, with absence of normal Doppler flow. MRI was subsequently performed to exclude septic joint. (B) Sagittal T2 FS, (C) Sagittal post-contrast T1 FS and (D) Axial post-contrast T1 FS images through the upper extremity confirm occluded proximal brachial vein (black arrows in B,C, and D), with thick enhancing peri-vascular and peri-neural soft tissue edema consistent with phlegmon. The brachial plexus branches run medial to the brachial vein and artery, and are secondarily involved in this case (bracket in D). (Color version of figure is available online).

increased rates in patients with certain systemic diseases such as neurofibromatosis type 1.⁶⁷ The telltale MRI features of peripheral nerve sheath tumors have been well described in the literature including: the target sign, split-fat sign, fascicular sign, and string sign. These tumors typically present as well-defined, avidly enhancing ovoid masses with the long axis of the lesion contiguous with the entering and exiting parent nerve. The target sign refers to peripheral hyperintensity and central hypointensity on T2-weighted imaging which is a result of predominantly myxoid tissue peripherally and a greater proportion of fibrocollagenous tissue centrally (Fig. 28).^{6,25,65} While very helpful in identifying peripheral nerve sheath tumors, the aforementioned imaging findings, including the target sign, are not useful for distinguishing between schwannoma and neurofibroma. However, these lesions can be accurately distinguished from one another based on their relationships to the parent nerves. Schwannomas are encapsulated lesions that have been classically described as “eccentric” to the parent nerve without infiltration of nerve fascicles; this is in contradistinction to neurofibromas which are unencapsulated and directly infiltrate

nerve fascicles.^{25,65} Identifying tumors as benign or malignant is valuable for preoperative counseling as schwannoma and solitary neurofibroma resections are typically possible without nerve injury while complete resection required to treat a plexiform neurofibroma will result in permanent nerve damage. The imaging appearance of benign peripheral nerve sheath tumors can be variable with some lesions such as long-standing ancient schwannomas demonstrating nonuniform enhancement and cystic necrosis mimicking MPNST.⁶⁸ Plexiform neurofibromas are often disfiguring due to the diffuse enlargement of the afflicted nerve and its branches, an appearance which has been described as a “bag of worms” at gross pathology. While plexiform neurofibromas often demonstrate the target sign at MRI, they are much larger than solitary neurofibromas with infiltrating, lobulated margins and nonuniform enhancement (Figs. 29 and 30).⁶⁹

MPNSTs often lack specific imaging features and may be impossible to differentiate from other soft tissue sarcomas, which reinforces the importance of the clinical history, particularly in patients with neurofibromatosis type 1 who

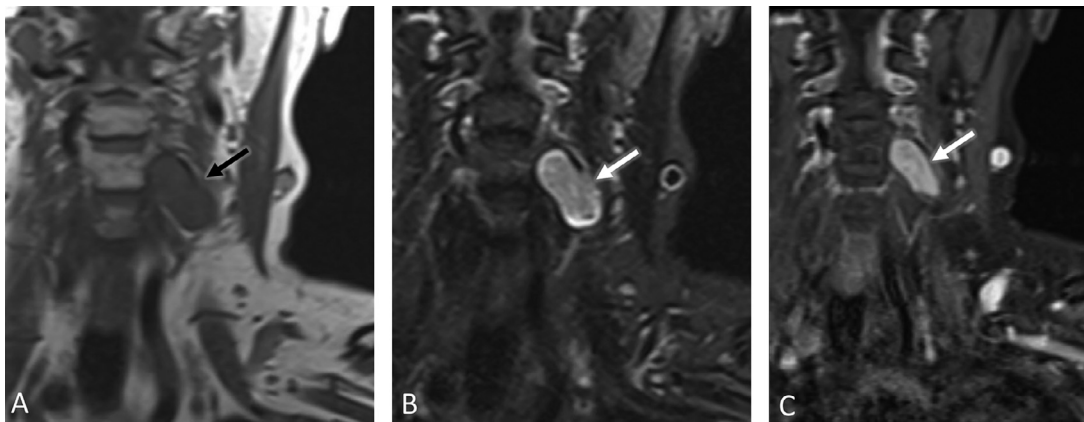


Figure 28 Peripheral Nerve Sheath Tumor. 57-year-old-woman with peripheral nerve sheath tumor arising from the exiting left C5 nerve root. (A) Coronal T1-weighted MR image shows a homogeneously hypointense dumbbell-shaped lesion slightly remodeling the left C4-C5 neural foramen (solid black arrow). (B) Coronal STIR MR image shows the classic “target sign” (solid white arrow) with peripheral hyperintensity and central hypointensity. (C) Coronal T1-weighted FS MR image following intravenous gadolinium administration shows diffuse, avid enhancement of the lesion (solid white arrow).

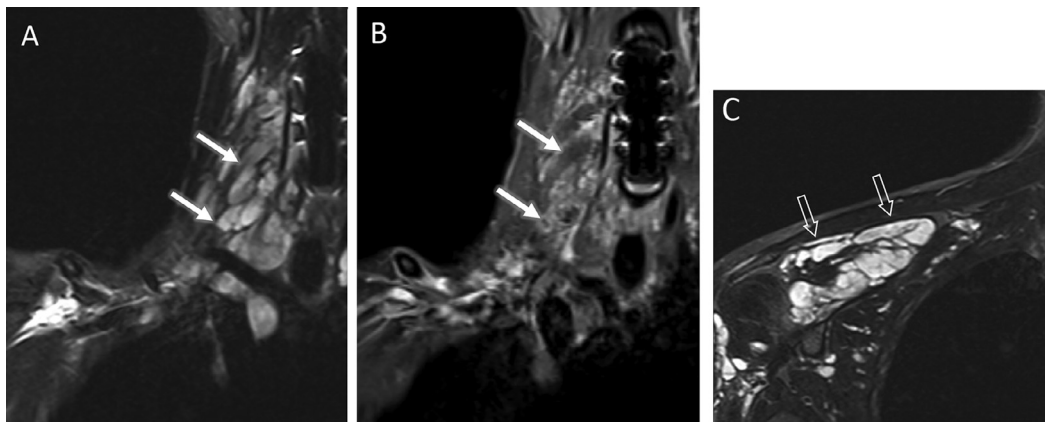


Figure 29 Neurofibromatosis. 29-year-old-woman with Neurofibromatosis Type-1 and multiple plexiform neurofibromas. (A) Coronal STIR MR image shows heterogeneous, predominately hyperintense lobulated enlargement of the right brachial plexus (solid white arrows). (B) Coronal T1-weighted FS MR image following intravenous gadolinium contrast administration shows non-uniform enhancement of the partially imaged brachial plexus (solid white arrows) involving the roots through divisions. (C) Coronal STIR MR image, at the level of the supraspinatus muscle belly, posterior to the brachial plexus, demonstrates an additional plexiform neurofibroma (open white arrows) with signal characteristics similar to the proximal brachial plexus lesions. There are numerous additional smaller hyperintense nodular foci throughout the right shoulder girdle soft tissues consistent with neurofibroma formation.

present with sudden increase in mass size, new onset pain or worsening neurologic deficits.⁷⁰ Several imaging features are useful in favoring a diagnosis of MPNST over benign peripheral nerve sheath tumors including: increasing size (greater than 7 cm), perilesional edema, peripheral enhancement, and intratumoral cystic change.⁶⁷ Local soft tissue invasion and osseous destruction are also highly suspicious for malignancy. FDG PET/CT avidity (standard uptake value >3-4) is suggestive of malignancy, but there is overlap in standard uptake values between MPNSTs and benign peripheral nerve sheath tumors with low uptake not excluding malignancy.⁷¹ ADC mapping has also been suggested as having a role for the diagnosis of MPNSTs, however is not currently used for diagnosis at our institution.

Non-Neurogenic Brachial Plexus Malignancies

Non-neurogenic brachial plexus malignancies may be further classified as tumors which secondarily invade the brachial plexus, and are more commonly seen than primary malignancies arising from the brachial plexus. The most common tumors to secondarily involve the brachial plexus include lung and breast cancer metastases, metastatic lymphadenopathy in the supraclavicular or axillary regions, neurolymphomatosis, and superior sulcus non-small cell lung carcinomas or Pancoast tumors.^{6,25,65} In general, these lesions may be focal or diffusely infiltrative with solid enhancement and invasion of regional osseous and soft tissue structures. In the setting of a superior sulcus tumor, patients typically present with Pancoast's

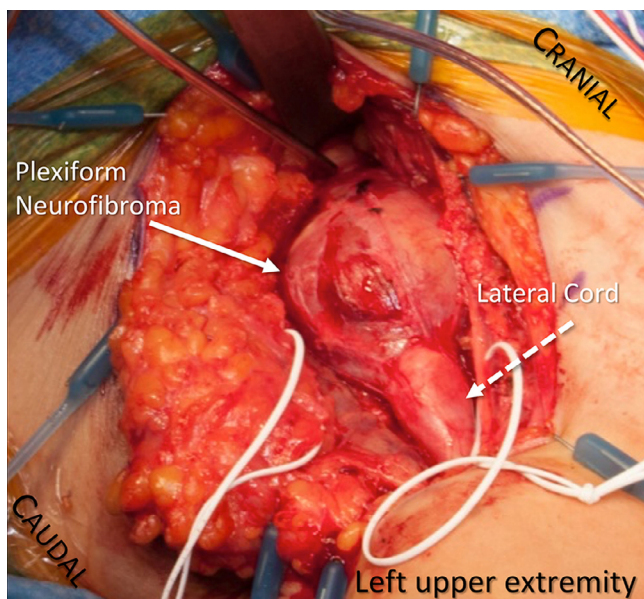


Figure 30 Plexiform Neurofibroma – Intra-operative view. Intra-operative picture during a NST resection demonstrates a fusiform shaped, multi-nodular tumor (solid white arrow) associated with the lateral cord. The lateral cord segment is expanded and diffusely enlarged (dashed white arrow).

syndrome, which includes hand musculature weakness and/or atrophy, shoulder and/or arm pain, and Horner's syndrome consisting of ptosis, anhidrosis, and miosis due to stellate ganglion invasion. When evaluating a superior sulcus tumor it is important to comment on involvement and/or invasion of the brachial plexus, subclavian vasculature, vertebral bodies and intervertebral foramina as contraindications to surgery include vertebral body infiltration of >50%, brachial plexus involvement cranial to C8, and extensive mediastinal involvement (tracheal or esophageal invasion)²⁵ (Fig. 31). Neurolymphoma is a rare extranodal manifestation of large B-cell non-Hodgkin lymphoma which has a predilection for the brachial plexus. The

diagnosis of neurolymphoma is challenging both clinically and at imaging with the MRI appearance of thickened, T2 hyperintense, enhancing peripheral nerves significantly overlapping with competing infectious and inflammatory etiologies.⁷¹ Given this limitation of MRI, FDG PET/CT has emerged as an invaluable complimentary modality demonstrating intense linear uptake of the involved nerves which is both highly specific and sensitive for lymphomatous infiltration. Any malignant bone tumor invading the scapula, vertebral bodies, first rib, or clavicle can secondarily involve the brachial plexus with osseous metastases being the most common culprit.⁶

Primary malignancies arising within the distribution of the brachial plexus include various soft tissue sarcomas including, but not limited to, liposarcoma, synovial sarcoma, undifferentiated pleomorphic sarcoma, as well as radiation-induced sarcoma. These lesions may have no particular differentiating features while others will have a similar appearance to those previously described in the literature arising remote from the brachial plexus (ie prominent adipose component in a well-differentiated liposarcoma).⁷² Radiation-induced sarcomas may occur as late as 40-years following radiation therapy, most often as the sequela of prior breast cancer therapy. Up to 11% of all MPNSTs have been associated with a history of prior therapeutic radiation.⁷³

Benign Non-Neurogenic Tumors

Multiple non-neurogenic benign tumors have been described arising in close proximity to the brachial plexus. The most commonly reported lesion is aggressive fibromatosis or desmoid tumor, which typically presents with pain or neurologic symptoms.⁶⁵ Similar to desmoids arising remote from the brachial plexus, these lesions are typically infiltrative with fascial tails and avid enhancement with predominant T1-hypointensity and T2-hyperintensity, but heterogeneous signal characteristics. Band-like T1 and T2-hypointense, nonenhancing regions of signal abnormality are the result of collagenous tissue deposition and suggestive of a fibrous neoplasm (Fig. 32).

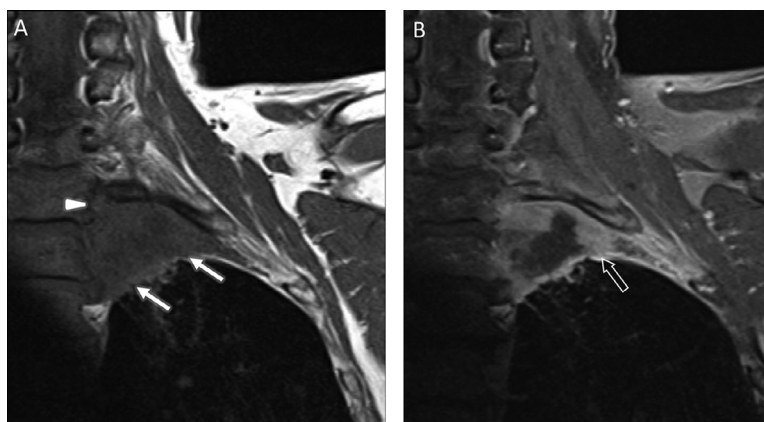


Figure 31 Malignant Tumor Invasion. 61-year-old man with non-small cell lung cancer and a left apical Pancoast tumor. (A) Coronal T1-weighted MR image shows a large destructive / locally invasive hypointense left superior sulcus tumor (solid white arrows) infiltrating the C8 and T1 nerve roots and inferior trunk of the brachial plexus (white arrowhead). (B) Coronal T1-weighted FS MR image following intravenous gadolinium administration shows thick, irregular peripheral enhancement of the lesion (open white arrow) with central necrosis.

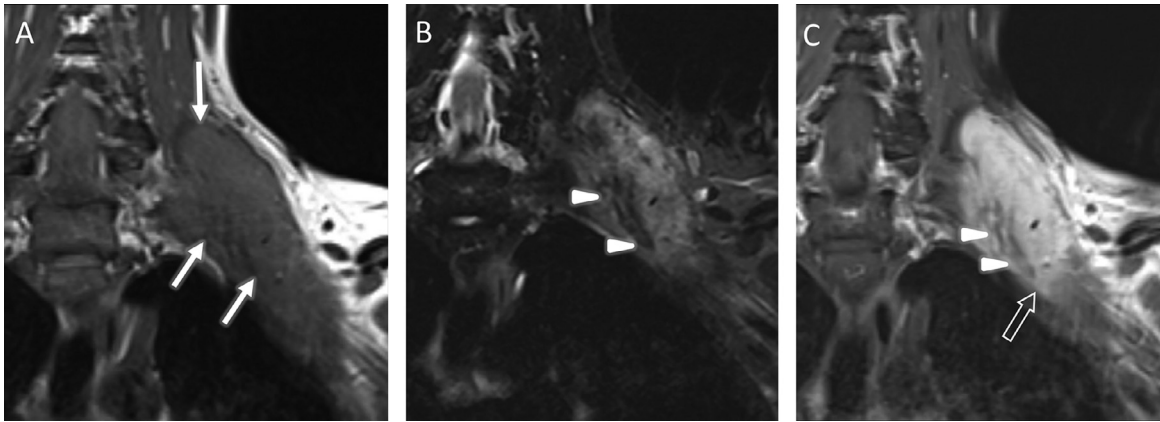


Figure 32 Infiltrating supra-clavicular desmoid tumor. 32-year-old female presents with a supra-clavicular desmoid tumor. (A) Coronal T1-weighted MR image shows a large, infiltrative hypointense mass diffusely involving the supra-clavicular through retroclavicular brachial plexus (solid white arrows). (B) Coronal STIR MR image shows heterogeneous, but primarily hyperintense signal intensity of the infiltrating mass with intralesional hypointense bands, which are characteristic of fibrous neoplasms (solid white arrowheads). (C) Coronal T1-weighted FS MR image following intravenous gadolinium contrast administration shows avid enhancement of the lesion with central non-enhancing, hypointense bands (solid white arrowheads). Enhancing fascial tail-like components (open white arrow) are characteristic of desmoid tumors.

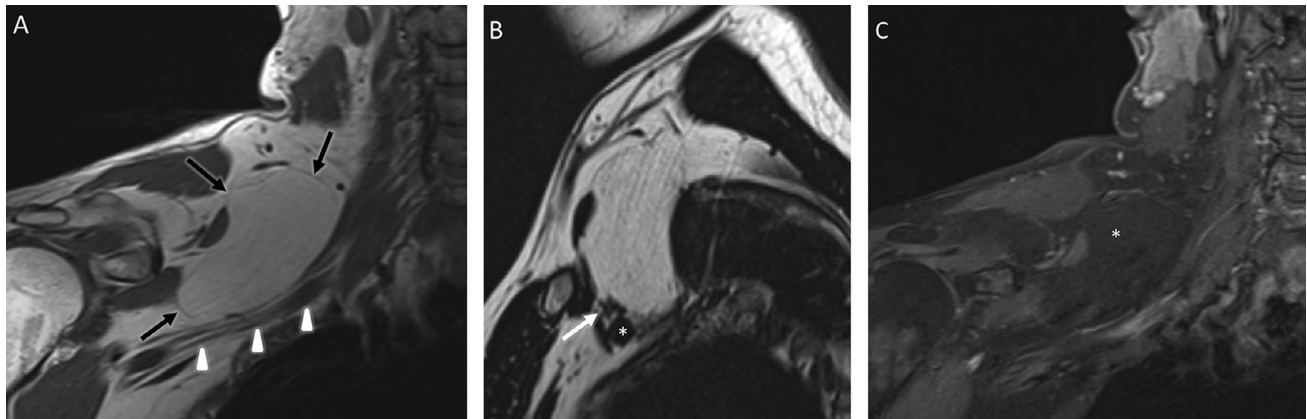


Figure 33 Lipoma. 62-year-old-man with right base of neck lipoma. (A) Coronal T1-weighted MRI shows a large, encapsulated fat containing lesion (black arrows) displacing the brachial plexus (arrowheads). (B) Sagittal T1-weighted MR image shows the fatty mass inferiorly displacing the cords of the brachial plexus (white arrow) and subclavian artery (asterisk). (C) Coronal T1-weighted FS MR image following intravenous gadolinium contrast administration shows diffuse signal loss within the fat containing lesion (asterisk) without intralesional enhancement.

While benign, these tumors are often locally aggressive and difficult to manage with high rates of recurrence.⁷⁴

The second most common benign non-neurogenic tumor to involve the brachial plexus is a lipoma. Lipomas are typically well characterized on CT and MRI given the diffuse simple intralesional fat (Fig. 33). However, it may be difficult to impossible to distinguish lipoma variants or lipomas which have undergone fat necrosis from atypical lipomatous tumor and/or well-differentiated liposarcoma.⁷⁵

There are reports of multiple other benign soft tissue and osseous tumors resulting in a brachial plexopathy including hemangioma, osteochondroma (Fig. 34), intraneural ganglion, and lymphangioma.²⁵

Conclusion

MR imaging of the brachial plexus need not be intimidating. Accurate interpretation of brachial plexus MRI is founded upon a solid understanding of normal anatomy, which can be further simplified by using an anatomical landmark-based approach to systematically interrogate each individual component of the brachial plexus. Combining this approach with an understanding of the common direct and indirect imaging findings and in concert with the clinical history and physical examination will allow the reader to identify the salient findings and arrive at the correct diagnosis.



Figure 34 Osteochondroma with brachial plexus impingement. 31-year-old man with a proximal humeral osteochondroma with superimposed non-united fracture. Coronal CT reformat through the right shoulder shows a non-united fracture of a pedunculated osteochondroma arising from the medial aspect of the proximal humeral metaphysis. The fracture fragment displaces the proximal peripheral branches of the brachial plexus (arrowheads).

Declaration of Interest

Nothing

References

- Belzberg AJ, Dorsi MJ, Storm PB, et al: Surgical repair of brachial plexus injury: A multinational survey of experienced peripheral nerve surgeons. *J Neurosurg* 101:365-376, 2004
- Kaiser R, Waldauf P, Haninec P: Types and severity of operated supraclavicular brachial plexus injuries caused by traffic accidents. *Acta Neurochir (Wien)* 154:1293-1297, 2012
- Nagano A: Treatment of brachial plexus injury. *J Orthop Sci* 3:71-80, 1998
- Rehman I, Chokshi FH, Khosa F: MR imaging of the brachial plexus. *Clin Neuroradiol* 24:207-216, 2014
- Yoshikawa T, Hayashi N, Yamamoto S, et al: Brachial plexus injury: Clinical manifestations, conventional imaging findings, and the latest imaging techniques. *Radiographics* 26:S133-S143, 2006
- Chhabra A, Thawait GK, Soldatos T, et al: High-resolution 3T MR neurography of the brachial plexus and its branches, with emphasis on 3D imaging. *AJNR Am J Neuroradiol* 34:486-497, 2013
- Torres C, Mailley K, Del Carpio O'Donovan R: MRI of the brachial plexus: modified imaging technique leading to a better characterization of its anatomy and pathology. *Neuroradiol J* 26:699-719, 2013
- Del Grande F, Santini F, Herzka DA, et al: Fat-suppression techniques for 3-T MR imaging of the musculoskeletal system. *Radiographics* 34:217-233, 2014
- Wang X, Harrison C, Mariappan YK, et al: MR neurography of brachial plexus at 3.0 T with robust fat and blood suppression. *Radiology* 283:538-546, 2017
- Chhabra A, Soldatos T, Subhawong TK, et al: The application of three-dimensional diffusion-weighted PSIF technique in peripheral nerve imaging of the distal extremities. *J Magn Reson Imaging* 34:962-967, 2011
- Takahara T, Hendrikse J, Yamashita T, et al: Diffusion-weighted MR neurography of the brachial plexus: Feasibility study. *Radiology* 249:653-660, 2008
- Zare M, Faeghi F, Hosseini A, et al: Comparison between three-dimensional diffusion-weighted PSIF technique and routine imaging sequences in evaluation of peripheral nerves in healthy people. *Basic Clin Neurosci* 9:65-71, 2018
- Vargas MI, Viallon M, Nguyen D, et al: New approaches in imaging of the brachial plexus. *Eur J Radiol* 74:403-410, 2010
- Bendszus M, Koltzenburg M, Wessig C, et al: Sequential MR imaging of denervated muscle: Experimental study. *AJNR Am J Neuroradiol* 23:1427-1431, 2002
- McDonald CM, Carter GT, Fritz RC, et al: Magnetic resonance imaging of denervated muscle: Comparison to electromyography. *Muscle Nerve* 23:1431-1434, 2000
- Kamath S, Venkatanarasimha N, Walsh MA, et al: MRI appearance of muscle denervation. *Skeletal Radiol* 37:397-404, 2008
- Chhabra A, Andreisek G, Soldatos T, et al: MR neurography: Past, present, and future. *AJR Am J Roentgenol* 197:583-591, 2011
- Ochi M, Ikuta Y, Watanabe M, et al: The diagnostic value of MRI in traumatic brachial plexus injury. *J Hand Surg Br* 19:55-59, 1994
- Tharin BD, Kini JA, York GE, et al: Brachial plexopathy: A review of traumatic and nontraumatic causes. *AJR Am J Roentgenol* 202:W67-W75, 2014
- Husarik DB, Saupe N, Pfirrmann CW, et al: Elbow nerves: MR findings in 60 asymptomatic subjects—normal anatomy, variants, and pitfalls. *Radiology* 252:148-156, 2009
- Blair DN, Rapoport S, Sostman HD, et al: Normal brachial plexus: MR imaging. *Radiology* 165:763-767, 1987
- Vijayarathna A, Chokshi FH: MRI of the brachial plexus: A practical review. *Appl Radiol* 45:9-18, 2016
- Doi K, Otsuka K, Okamoto Y, et al: Cervical nerve root avulsion in brachial plexus injuries: Magnetic resonance imaging classification and comparison with myelography and computerized tomography myelography. *J Neurosurg* 96:277-284, 2002
- Sureka J, Cherian RA, Alexander M, et al: MRI of brachial plexopathies. *Clin Radiol* 64:208-218, 2009
- van Es HW, Bollen TL, van Heeswijk HP: MRI of the brachial plexus: A pictorial review. *Eur J Radiol* 74:391-402, 2010
- Narakas AO: The treatment of brachial plexus injuries. *Int Orthop* 9:29-36, 1985
- Martinoli C, Gandolfo N, Perez MM, et al: Brachial plexus and nerves about the shoulder. *Semin Musculoskelet Radiol* 14:523-546, 2010
- Hayashi N, Yamamoto S, Okubo T, et al: Avulsion injury of cervical nerve roots: Enhanced intradural nerve roots at MR imaging. *Radiology* 206:817-822, 1998
- Carvalho GA, Nikkhah G, Matthies C, et al: Diagnosis of root avulsions in traumatic brachial plexus injuries: Value of computerized tomography myelography and magnetic resonance imaging. *J Neurosurg* 86:69-76, 1997
- Gasparotti R, Ferraresi S, Pinelli L, et al: Three-dimensional MR myelography of traumatic injuries of the brachial plexus. *AJNR Am J Neuroradiol* 18:1733-1742, 1997
- Bendszus M, Koltzenburg M: Visualization of denervated muscle by gadolinium-enhanced MRI. *Neurology* 57:1709-1711, 2001
- Chhabra A, Williams EH, Wang KC, et al: MR neurography of neuromas related to nerve injury and entrapment with surgical correlation. *AJNR Am J Neuroradiol* 31:1363-1368, 2010
- Titelbaum DS, Frazier JL, Grossman RI, et al: Wallerian degeneration and inflammation in rat peripheral nerve detected by in vivo MR imaging. *AJNR Am J Neuroradiol* 10:741-746, 1989
- Yamabe E, Nakamura T, Oshio K, et al: Peripheral nerve injury: Diagnosis with MR imaging of denervated skeletal muscle—experimental study in rats. *Radiology* 247:409-417, 2008
- Seddon HJ: Three types of nerve injury. *Brain* 66:237-288, 1943
- Sakellariou VI, Badilas NK, Mazis GA, et al: Brachial plexus injuries in adults: Evaluation and diagnostic approach. *ISRN Orthop* 2014:726103, 2014
- Robertson WC Jr., Eichman PL, Clancy WG: Upper trunk brachial plexopathy in football players. *JAMA* 241:1480-1482, 1979
- Levitz CL, Reilly PJ, Torg JS: The pathomechanics of chronic, recurrent cervical nerve root neuropathy. The chronic burner syndrome. *Am J Sports Med* 25:73-76, 1997
- Medina LS, Yaylali I, Zurakowski D, et al: Diagnostic performance of MRI and MR myelography in infants with a brachial plexus birth injury. *Pediatr Radiol* 36:1295-1299, 2006
- Menashe SJ, Tse R, Nixon JN, et al: Brachial plexus birth palsy: Multimodality imaging of spine and shoulder abnormalities in children. *AJR Am J Roentgenol* 204:W199-W206, 2015
- Smith AB, Gupta N, Strober J, et al: Magnetic resonance neurography in children with birth-related brachial plexus injury. *Pediatr Radiol* 38:159-163, 2008

42. Thatte MR, Mehta R: Obstetric brachial plexus injury. *Indian J Plast Surg* 44:380-389, 2011
43. Van Gelein Vitringa VM, Jaspers R, Mullender M, et al: Early effects of muscle atrophy on shoulder joint development in infants with unilateral birth brachial plexus injury. *Dev Med Child Neurol* 53:173-178, 2011
44. al-Qattan MM, Clarke HF, Curtis CG: Klumpke's birth palsy. Does it really exist? *J Hand Surg* 20B:19-23, 1995
45. Buchanan EP, Richardson R, Tse R: Isolated lower brachial plexus (Klumpke) palsy with compound arm presentation: Case report. *J Hand Surg Am* 38:1567-1570, 2013
46. Borschel GH, Clarke HM: Obstetrical brachial plexus palsy. *Plast Reconstr Surg* 124:144e-155e, 2009
47. Waters PM: Comparison of the natural history, the outcome of microsurgical repair, and the outcome of operative reconstruction in brachial plexus birth palsy. *J Bone Joint Surg Am* 81:649-659, 1999
48. Delanian S, Lefaix JL, Pradat PF: Radiation-induced neuropathy in cancer survivors. *Radiother Oncol* 105:273-282, 2012
49. Kori SH, Foley KM, Posner JB: Brachial plexus lesions in patients with cancer: 100 cases. *Neurology* 31:45-50, 1981
50. Wittenberg KH, Adkins MC: MR imaging of nontraumatic brachial plexopathies: Frequency and spectrum of findings. *Radiographics* 20:1023-1032, 2000
51. Bowen BC, Verma A, Brandon AH, et al: Radiation-induced brachial plexopathy: MR and clinical findings. *AJNR Am J Neuroradiol* 17:1932-1936, 1996
52. Demondion X, Herbinet P, Van Sint Jan S, et al: Imaging assessment of thoracic outlet syndrome. *Radiographics* 26:1735-1750, 2006
53. Urschel HC Jr., Razzuk MA: Neurovascular compression in the thoracic outlet: Changing management over 50 years. *Ann Surg* 228:609-617, 1998
54. Magill ST, Brus-Ramer M, Weinstein PR, et al: Neurogenic thoracic outlet syndrome: Current diagnostic criteria and advances in MRI diagnostics. *Neurosurg Focus* 39:E7, 2015
55. Feinberg JH, Radecki J: Parsonage-turner syndrome. *HSS J* 6:199-205, 2010
56. Zara G, Gasparotti R, Manara R: MR imaging of peripheral nervous system involvement: Parsonage-Turner syndrome. *J Neurol Sci* 315:170-171, 2012
57. Mathey EK, Pollard JD: Chronic inflammatory demyelinating polyneuropathy. *J Neurol Sci* 333:37-42, 2013
58. Koller H, Kieseier BC, Jander S, et al: Chronic inflammatory demyelinating polyneuropathy. *N Engl J Med* 352:1343-1356, 2005
59. Mygland A, Monstad P, Vedeler C: Onset and course of chronic inflammatory demyelinating polyneuropathy. *Muscle Nerve* 31:589-593, 2005
60. Van Es HW, Van den Berg LH, Franssen H, et al: Magnetic resonance imaging of the brachial plexus in patients with multifocal motor neuropathy. *Neurology* 48:1218-1224, 1997
61. Shibuya K, Sugiyama A, Ito S, et al: Reconstruction magnetic resonance neurography in chronic inflammatory demyelinating polyneuropathy. *Ann Neurol* 77:333-337, 2015
62. Dimitropoulou D, Lagadinou M, Papayiannis T, et al: Septic thrombophlebitis caused by fusobacterium necrophorum in an intravenous drug user. *Case Rep Infect Dis* 2013:870846, 2013
63. Miron D, Bor N, Cutai M, et al: Transient brachial palsy associated with suppurative arthritis of the shoulder. *Pediatr Infect Dis J* 16:326-327, 1997
64. White HD, White BA, Boethel C, et al: Pancoast's syndrome secondary to infectious etiologies: A not so uncommon occurrence. *Am J Med Sci* 341:333-336, 2011
65. Saifuddin A: Imaging tumours of the brachial plexus. *Skeletal Radiol* 32:375-387, 2003
66. Louis DN, Ohgaki H, Wiestler OD, et al: The 2007 WHO classification of tumours of the central nervous system. *Acta Neuropathol* 114:97-109, 2007
67. Wasa J, Nishida Y, Tsukushi S, et al: MRI features in the differentiation of malignant peripheral nerve sheath tumors and neurofibromas. *AJR Am J Roentgenol* 194:1568-1574, 2010
68. Isobe K, Shimizu T, Akahane T, et al: Imaging of ancient schwannoma. *AJR Am J Roentgenol* 183:331-336, 2004
69. Wilkinson LM, Manson D, Smith CR: Best cases from the AFIP: Plexiform neurofibroma of the bladder. *Radiographics* 24:S237-S242, 2004
70. Karsy M, Guan J, Ravindra VM, et al: Diagnostic quality of magnetic resonance imaging interpretation for peripheral nerve sheath tumors: Can malignancy be determined? *J Neurol Surg Part A, Central Eur Neurosurg* 77:495-504, 2016
71. Crush AB, Howe BM, Spinner RJ, et al: Malignant involvement of the peripheral nervous system in patients with cancer: Multimodality imaging and pathologic correlation. *Radiographics* 34:1987-2007, 2014
72. Murphey MD, Arcara LK, Fanburg-Smith J: From the archives of the AFIP: Imaging of musculoskeletal liposarcoma with radiologic-pathologic correlation. *Radiographics* 25:1371-1395, 2005
73. Ducatman BS, Scheithauer BW, Piepgras DG, et al: Malignant peripheral nerve sheath tumors. A clinicopathologic study of 120 cases. *Cancer* 57:2006-2021, 1986
74. Dinauer PA, Brixey CJ, Moncur JT, et al: Pathologic and MR imaging features of benign fibrous soft-tissue tumors in adults. *Radiographics* 27:173-187, 2007
75. Khashper A, Zheng J, Nahal A, et al: Imaging characteristics of spindle cell lipoma and its variants. *Skeletal Radiol* 43:591-597, 2014